UNIVERSIDADE DE LISBOA
FACULDADE DE CIÊNCIAS
DEPARTAMENTO DE QUÍMICA E BIOQUÍMICA

Investigation of Quinone Reductases from *Staphylococcus aureus*

Patrícia Matos Pires

Mestrado em Bioquímica
Especialização em Bioquímica Médica

Dissertação orientada por:
Manuela M. Pereira

2019

Agradecimentos

Em primeiro lugar gostaria de agradecer à minha orientadora a Dra. Manuela Pereira por me ter proporcionado esta oportunidade e por sempre me guiar, aconselhar e ajudar, com essa força e positivismo que lhe são característicos, em tudo o que precisava neste projeto.

À Universidade de Lisboa, à FCUL e ao BioISI por me terem proporcionado todas as condições necessárias para a realização da minha dissertação. A todos, que direta ou indiretamente me ajudaram ao longo do decorrer da minha dissertação. Um obrigado especial a professora Ana Coutinho, pelo tempo despendido comigo a ajudar-me, à professora Helena Gaspar pela disponibilidade do seu equipamento de HPLC e ao professor Rodrigo Almeida e ao seu grupo pela ajuda e disponibilidade do espectroflurímetro.

Um grande obrigado também aos grupos de investigação Protein *Folding and Misfolding Laboratory*, ao grupo *FunGP – Functional Genomics and Proteostasis* e *RNA Biology and Bioinformatics lab* pela disponibilidade de equipamentos e pela ajuda prestada.

Queria deixar um enorme obrigado a todo o grupo do *Bioenergetics Lab*, Filipe Sousa, Patrícia Refojo, Filipa Sena, Filipa Calisto, Tatiana Pires e Diana Duarte, por toda a amizade, motivação, ajuda e apoio prestado.

À Filipa Sena por ser um exemplo de força, garra e determinação tanto a nível profissional como a nível pessoal e por sempre me fazer perceber que tudo tem uma solução e o importante é sermos felizes.

Ao Filipe por equilibrar o grupo, descomplicar, nos fazer pensar e por estar sempre pronto a ajudar.

À Patrícia por acreditar em mim, por me ter proporcionado trabalhar com ela numa área que tanto gosto e me fazer ver que é importante sermos bons profissionais, mas que o essencial é nos divertirmos a trabalhar.

À Tatiana por me ter acompanhado nesta aventura que é trabalhar na nossa dissertação e por estar sempre pronta a ajudar e me fazer ver que se quisermos somos todos capazes de fazer tudo a que nos dispomos.

À Diana por ver sempre o lado positivo de tudo, por me fazer rir e me tentar passar a sua atitude zen.

Um muito obrigado também ao ITQB e aos grupos de investigação da professora Mariana Pinho, *Bacterial Cell Biology*, e do professor Miguel Teixeira, *Metalloenzymes and Molecular Bioenergetics*, por me proporcionarem a possibilidade de trabalhar nos vossos laboratórios. Um especial agradecimento ao João Carita e Pedro Fernandes que sempre se mostraram disponíveis para me ajudar.

A todos o que conheci ao longo do meu percurso académico e que se foram tornando amigos que sempre fizeram a diferença. Um meu muito obrigado ao Pedro Barbosa, Ana Mortinho e Sara Jorge por me fazerem rir muito, me apoiarem, me aturarem nos momentos bons e maus e não me deixarem desistir, mesmo quando tinha as minhas crises existenciais.

Aos meus colegas de mestrado por terem tornado tudo mais fácil e por termos passado por esta etapa juntos.

Um agradecimento muito, muito especial à minha família, em especial à minha mãe, pai e irmã por tudo o que fizeram por mim, por sempre estarem do meu lado, apoiarem-me em tudo e nunca me deixarem desistir. Por me mostrarem o que é ser - se determinado, perseverante, forte, lutador, pela minha educação, valores e por tudo o que sou hoje em dia.

À minha avó, que infelizmente perdi neste ano, mas que sei que mesmo não entendendo em que é que eu trabalho sentia na mesma um orgulho imenso da sua neta.

Resumindo, agradeço por todos os momentos, alegrias, decepções, lições e aprendizagens que todos de um modo diferente e único de cada um me proporcionaram e me fizeram crescer e aprender muita coisa com vocês.

O meu muito Obrigado!

Abstract

Staphylococcus aureus is a major human opportunistic pathogen that causes a wide range of clinical infections. Methicillin-resistant *Staphylococcus aureus* (MRSA) have been considered a serious and worldwide problem to public health.

The variable metabolic capacities allow *S. aureus* to adapt to different conditions. However and surprisingly the respiratory chain of *S. aureus* is quite simple, and the metabolism of this pathogen is still very little explored.

This thesis focused on the expression and purification of the Dihydroorotate:quinone oxidoreductase from *Staphylococcus aureus;* and biochemical and cellular characterization of three quinone reductases from the respiratory chain of the same organism: Dihydroorotate:quinone oxidoreductase (DHOQO), Glycerol-3-phosphate:quinone oxidoreductase (G3PQO) and Pyruvate:quinone oxidoreductase (PQO). These proteins catalyze the oxidation of the different substrates (electron donors) and the reduction of the quinone (electron acceptor) to a quinol form, providing electrons to the respiratory chain.

In this work, the expression and purification of DHOQO from *S. aureus* was achieved and successful biochemical and cellular characterizations of DHOQO, G3PQO and PQO were performed.

From the protein biochemical point of view, G3PQO and PQO are identified as dimeric enzymes, presenting FAD as cofactor. By contrast, the monomeric protein, DHOQO was shown to have an FMN molecule as a cofactor and it was shown to be purified in a redox active state. Protein substrate interaction studies showed that the three proteins under study have higher affinity to DMN, a menaquinone analogue (which is the physiological quinone found in the membranes of *Staphylococcus aureus*). These studies also suggested that the binding of quinone and dihydroorotate (the electron donor of DHOQO) seem to take place at different binding sites, since the presence of the inhibitor HQNO only affected the interaction of the protein with the quinone.

For a cellular role characterization, we aimed to construct knockout mutants for the three quinone reductases. The knockout mutant of the DHOQO (ΔDHOQO) was successfully obtained and growth studies of ΔDHOQO revealed that DHOQO is relevant and impacting in the metabolism of the *S. aureus.*

Keywords: *Staphylococcus aureus*; Dihydroorotate:quinoneoxidoreductase; Glycerol-3-phosphate:quinone oxidoreductase; Pyruvate:quinone oxidoreductase; Δ DHOQO

Resumo

Staphylococcus aureus é um dos maiores patógenos oportunistas, sendo responsável por um grande número de infeções. Atualmente, as estirpes de *S. aureus* resistentes à meticilina (MRSA) são consideradas um grande problema de saúde pública, tanto no controlo da infeção como no seu tratamento. Na verdade, *S. aureus* é uma das causas mais comuns de infeções em ambiente hospitalar. Por esta razão, não só é importante explorar e perceber os mecanismos por de trás dessa múltipla resistência a antibióticos, mas também compreender melhor os fatores que permitem a este microrganismo viver e sobreviver em diferentes condições.

A diversidade metabólica deste organismo permite-lhe sobreviver em diferentes ambientes, fazendo deste um patógeno tão perigoso. Apesar disso e surpreendentemente, a cadeia respiratória deste organismo é muito simples e o seu metabolismo é pouco explorado. Enzimas constituintes da cadeia respiratória apesar de ser identificadas como *drug target* em diferentes patologias como é o caso da malária, continuam a ser muito pouco estudadas. No caso das enzimas da cadeia respiratória de *S.aureus* pouca informação pode ser encontrada sobre estas proteínas na literatura.

Por isso este trabalho aqui desenvolvido no âmbito desta dissertação pretende contribuir para o alargamento do conhecimento acerca do metabolismo energético desta bactéria. Este projeto de dissertação focou-se na expressão e purificação da Dihidroorotato: quinona oxidorreductase de *S. aureus*; e na caracterização bioquímica e celular de três quinonas redutases expressas pelo mesmo organismo e que estão envolvidas em diferentes vias metabólicas de produção de energia, a Dihidroorotato: quinona oxidorreductase (DHOQO); a Glicerol-3-fosfato: quinona oxidorreductase (G3PQO) e a Piruvato: quinona oxidorreductase (PQO). Estas enzimas catalisam a oxidação de diferentes substratos e a redução da quinona a quinol, fornecendo eletrões à cadeia respiratória.

Estas proteínas são caracterizadas como flavoproteínas uma vez que apresentam flavina como cofator, o que lhes confere não só o espectro UV-visível característico das flavoproteínas com bandas a 375 nm e a 450 nm, mas também a cor amarela às amostras que contêm as proteínas de interesse. A DHOQO, G3PQO e a PQO são também classificadas como enzimas monotópicas, uma vez que estão apenas presentes num lado da membrana e se encontram ligadas a esta através de interações eletrostáticas.

A DHOQO é uma enzima que catalisa a oxidação do dihidroorotato a orotato, sendo os eletrões transferidos para a quinona, através do seu cofator FMN. Esta reação enzimática é a única reação de oxidação-redução e corresponde ao quarto passo da via de biossíntese das pirimidinas. A DHOQO expressa em *S. aureus* é codificada pelo gene *pyrD* e tem a massa molecular teórica de 39 kDa.

No caso da G3PQO, esta catalisa a oxidação do glicerol 3-fosfato a dihidroxiacetona fosfato com transferência de eletrões para a quinona. Em *S. aureus* esta enzima é codificada pelo gene *glpD* e é uma enzima com 62 kDa.

Ao contrário das outras duas quinona redutases, a PQO apresenta além da flavina, o TPP e o Mg^{2+} como cofatores, catalisando a descarboxilação oxidativa do piruvato a acetato e CO_2 com transferência de eletrões para a quinona. A PQO expressa em *S. aureus* é uma enzima com 63 kDa e que é codificada pelo gene *CidC.*

Neste trabalho expressámos e purificámos a DHOQO com sucesso, tendo-se feito a caracterização bioquímica e celular da DHOQO, G3PQO e PQO. Além da caracterização bioquímica, o estudo da DHOQO foi complementado ao nível celular através da comparação do crescimento da estirpe *wild type* e estirpe mutante *knockout* da proteína DHOQO. Estas três proteínas em estudo foram caracterizadas espectroscopicamente tendo sido também testada a sua estabilidade térmica e investigado o seu estado de oligomerização. O respetivo grupo prostético foi também identificado. No caso da DHOQO, esta foi funcionalmente caracterizada através de estudos cinéticos, do perfil de pH e de estudos de interação de proteína substratos.

A G3PQO e a PQO foram identificadas como enzimas diméricas e que apresentam FAD como cofator. Pelo contrário, a proteína monomérica DHOQO tem como cofator FMN e mostrou ter atividade de dihidroorotato:quinona oxidorreductase, sendo inibida pela presença em solução de HQNO (conhecido inibidor de quinonas redutases).

Ensaios de quenching de fluorescência foram feitos para o estudo da interação de proteína e substratos (DMN, duroquinona, os respetivos dadores de eletrões e HQNO). Nestes estudos os resíduos de triptofanos são excitados a 295 nm, sendo observada uma diminuição na emissão de fluorescência dos mesmos. O *quenching* observado na emissão da proteína deve-se a mudança de ambiente químico dos resíduos de triptofanos causado pela mudança de conformação das proteínas induzida pela interação da enzima e do substrato.

Os nossos dados experimentais mostraram que as três quinona redutases apresentam uma maior afinidade para a menaquinona (DMN) do que para a duroquinona (Benzoquinona), estes dados estão de acordo com o facto de *S. aureus* sintetizar menaquinona naturalmente. Os mesmo estudos de *quenching* de fluorescência sugerem também que a ligação da quinona (DMN) e do dihidroorotato, no caso da DHOQO, parece ser feita em dois locais de ligação diferentes, uma vez que a presença do inibidor HQNO, afeta apenas a interação da quinona com a proteína.

Na caracterização celular, o objetivo principal foi a obtenção de mutantes *knockouts* da DHOQO, G3PQO e da PQO. Este processo de obtenção de mutantes envolve 5 passos principais: 1) amplificação dos fragmentos *up* e *down* (aproximadamente 1300 pares de bases *upstream* e 1300 pares de bases *downtream* do gene que codifica para a proteína de interesse, respetivamente); 2) Obtenção de fragmento *overlap* através de *overlapping* PCR; 3) Clonagem de fragmento *up-down* de cada proteína no vector de clonagem pMAD; 4) Electroporação em *S. aureus* RN4220; 5) Transdução de *S. aureus* MW2.

A recombinação e a integração do plasmídeo no genoma de *S. aureus* são obtidos através de um processo de recombinação homóloga que envolve dois passos principais, a integração e a excisão. No primeiro passo, os recombinantes são selecionados a uma temperatura não permissiva para a replicação do plasmídeo (43 ºC), usando eritromicina e a cor azul das colónias (devido a metabolização de X-gal). Num segundo passo, as células são incubadas a 30 ºC na ausência de seleção por antibiótico. Neste passo, as colónias brancas resultantes são aquelas em que o vector foi excisado com sucesso.

No caso da G3PQO e da PQO os mutantes *knockout* não foram obtidos, enquanto para a DHOQO foi obtido com sucesso. A obtenção destes mutantes para as três quinonas redutases permite-nos a investigação do papel e relevância destas proteínas no metabolismo deste perigoso patógeno, estudando assim o efeito da deleção destas proteínas no crescimento/ metabolismo energético de *S. aureus*. Para isso, crescimentos das estirpes *wild type* e mutada para a proteína DHOQO foram realizados. Durante os crescimentos foram monitorizadas a densidade celular óptica a 600 nm e o valor de pH. Crescimentos com estirpe *wild type* e a estirpe mutante da proteína DHOQO revelaram que DHOQO parece ter um papel relevante no metabolismo de *S. aureus*, uma vez que foram observadas diferenças tanto no crescimento como no perfil de pH das duas estirpes em estudo.

Palavras-chave: *Staphylococcus aureus*; Dihidroorotato: quinona oxidorreductase; Glycerol-3-fosfato: quinona oxidorreductase; Piruvato: quinona oxidorreductase; ΔDHOQO

Index

Index of figures

Index of tables

List of abbreviations

Abs- Absorbance
A280/A450- Ratio between the absorbance at 280 nm and 450 nm
CpI- Complex I
CpII- Complex II
CpIII- Complex III
CpIV- Complex IV
DMN- 2,3- Dimethyl-1,4-naphthoquinone
DUR- duroquinone
DHOQO- Dihydroorotate:quinone oxidoreductase
DHOQO KO- knockout mutant of DHOQO
Dihy-Dihydroorotate
Ery- Erythromycin
FAD- Flavin adenine dinucleotide
FMN- Flavin mononucleotide
G3P- Glycerol-3- phosphate
G3PQO- Glycerol-3- phosphate: quinone oxidoreductase
G3PQO KO- knockout mutant of G3PQO
HQNO- 2-n-Heptyl-4-hydroxyquinoline N-oxide
IPTG- isopropyl – β- D- thiogalactopyranoside
K_D- Dissociation constant
K_i- Inhibition constant
K_M- Michaelis- Menten constant
MRSA- Methicillin resistant *S. aureus*
$OD_{600\ nm}$ – Optical density at 600 nm
PVL- Panton- Valentine leukocidin
PCR- Polymerase Chain Reaction
PQO- Pyruvate: quinone oxidoreductase
PQO KO- knockout mutant of PQO
PSM- Phenol soluble modulins
Q- Quinone
QH_2- Quinol
SDS-PAGE- sodium dodecyl sulfate polyacrylamide gel electrophoresis
TB medium- Terrific broth medium
TSA- Tryptic soy agar
TSB- Tryptic soy broth
UV-vis- Ultra-violet visible
Vo- initial rate
Vmax- maximum rate
WT- wild type
X-Gal- 5-Bromo-4-chloro-3-indolyl β-D-galactopyranoside

1. Aims

This thesis aimed to contribute to extend the knowledge borders on the energetic metabolism of *Staphylococcus aureus* by studying monotopic proteins of its respiratory chain. Our main goals were:

- Expression and purification of the Dihydroorotate:quinone oxidoreductase from *Staphylococcus aureus*;

- Biochemical characterization of three quinone reductases from respiratory chain of *Staphylococcus aureus*, Dihydroorotate:quinone oxidoreductase, Glycerol-3-phosphate:quinone oxidoreductase and Pyruvate:quinone oxidoreductase

- Investigate the relevance and impact of those proteins in the metabolism of *Staphylococcus aureus* by the construction of knockouts mutants.

2. Introduction

2.1. Energetic metabolism

2.1.1. Energy

In living organisms, different types of energy are always interconverting in the cell in order to allow it to perform different functions. Cells use energy from external sources, such as organic or inorganic compounds or light, to sustain growth and reproduce themselves. Energy is mainly required for motility, to active transport of molecules and ions and to synthetize macromolecules from simple precursors [1][2]. The way cells deal with energy, how do they obtain it, convert it into different forms, store it or use it is the focus of Bioenergetics.

Metabolism is essentially a sum of the linked enzymatic reactions that occur in the living cells. Cellular metabolism includes catabolic reactions and anabolic reactions. Catabolism involves all the reactions that allow cells to obtain, convert and store energy from nutrients, in this way catabolic reactions are defined as all enzymatic reactions involved in the breakdown of organic or inorganic compounds in order to obtain and store energy. Using these types of reactions, the cell obtains and stores energy for example in the form of ATP. Anabolic reactions are defined as biosynthetic reactions that lead to the production of molecules such as proteins, DNA, RNA or lipids from small molecules using the energy obtained by the process of catabolism [3].

In vertebrates, energy is mainly obtained by oxidative phosphorylation in the mitochondria. The link between the oxidoreduction of substrates and ATP synthesis has been explained by the Chemiosmotic theory postulated by Peter Mitchell in 1961, proposing that free energy released from the oxidoreduction reactions of some substrates could be conserved through the establishment of a transmembrane difference of electrochemical potential described by the proton motive force. The proton motive force is composed of two different components: the difference in chemical concentrations between the two sides of the membrane, and the difference in the charge distribution between the two sides of the same membrane. The dissipation of the transmembrane difference of electrochemical potential through the ATP synthase provides the necessary energy for the synthesis of ATP [4] [5].

2.2. Canonical Respiratory Chain

The respiratory chain is composed of several enzymatic complexes that perform oxidoreduction reactions and, in some cases, translocate ions across the membrane against the electrochemical potential. The respiratory chains, as the mitochondrial one, are composed of several membrane proteins, which perform an oxidoreduction of metabolites toward the reduction of terminal electron acceptors. To survive in different environments and support different conditions, organisms present different respiratory chain proteins.

The canonical respiratory chain of mammals consists of four protein complexes: Complex I, II, III and IV and of the mobile electron carriers: ubiquinone and cytochrome *c* that facilitated the electron transfer between the complexes.

Complex I or NADH:ubiquinone oxidoreductase (EC:1.6.5.3) catalyzes the transfer of two electrons oxidation of NADH by quinone, coupled to the translocation of possibly four protons across the membrane contributing in this way to the establishment of the membrane potential. This complex is one of the largest components of the respiratory chain. The mammalian mitochondrial enzyme consists of 44 different subunits summing up to 1000 kDa and has as cofactors one Flavin Mononucleotide (FMN) and eight iron-sulfur clusters. Structurally, Complex I has a characteristic L-shaped structure, with the hydrophobic arm, the responsible for ion translocation, embedded in the membrane and the hydrophilic peripheral arm, in which the catalytic reaction takes place, extended into the mitochondrial matrix [6].

Complex II (CpII), also called Succinate:quinone oxidoreductase (EC: 1.3.5.1), is a membrane-anchored complex with a hydrophilic domain located in the cytoplasm. It is constituted by four subunits and catalyze the two-electron oxidation of succinate to fumarate with the reduction of ubiquinone to ubiquinol. This catalytic reaction is not coupled to the translocation of charges, as in case of complex I [7].

Complex III (Ubiquinol:cytochrome *c* oxidoreductase or cytochrome bc_1 complex; EC:1.10.2.2), catalyzes the electron transfer from ubiquinol to cytochrome *c*, coupled with the generation of the membrane potential. The mitochondrial bc_1 complex has 11 subunits per monomer but only cytochrome c_1, cytochrome *b* and the Rieske protein, the catalytic subunits, are conserved throughout the entire protein family [8].

The final step in electron transfer chain of mitochondria is catalyzed by complex IV (EC:1.9.3.1), also called cytochrome *c* oxidase or cytochrome *c*:oxygen oxidoreductase. In this reaction O_2 is reduced to H_2O and four protons are pumped across the membrane. This complex consists of 13 subunits but only two of them are involved in catalysis and proton translocation [1].

The energetic metabolism of prokaryotes is much more diverse as a consequence of the different conditions and environments where prokaryotes can live. These organisms may use different organic or inorganic compounds as external energy sources and several electron acceptors, such as oxygen, iron, sulfur/nitrogen compounds, or organic metabolites. Because of that, their respiratory chains, presents a large variety of complexes, showing remarkable diversity, flexibility and robustness in comparation with the mammalian one [9].

2.3. Staphylococcus aureus

2.3.1. General characteristics

Staphylococcus aureus is a facultative anaerobic, Gram-positive, nonsporulating, cocci bacterium, member of the Firmicutes phylum. These bacteria are present in the microbiota of the human body, frequently found in the upper respiratory tract and on the skin.

Although *Staphylococcus aureus* is a commensal bacterium, this organism is a major human opportunistic pathogen and causes a wide range of clinical infections, such as bacteremia and infective endocarditis as well as osteoarticular, skin, soft tissue, pleuropulmonary, and device-related infections, in which the bacterial toxins are important mediators [10].

2.3.2. Virulence factors

Staphylococcus aureus strains, more specifically, methicillin-resistant *Staphylococcus aureus* (MRSA) have been considered a serious and worldwide problem to public health.

The rise of antibiotic-resistant strains in the 1960s and 1970s has created additional therapeutic challenges. During infection, impaired functions are caused by host tissue damage induced by various virulence factors released upon bacterial replication. The bacterial toxins specifically trigger the immune system, resulting in subsequent cytokine release and tissue injury.

The PVL (Panton-Valentine leucocidin), α-toxin, PSM (phenol-soluble modulins) and superantigens are examples of toxins secreted by *S. aureus*. These toxins are able to recruit, activate and lysate human immune cells such as neutrophils, leukocytes, lymphocytes and macrophages. The α-toxin also alters platelet morphology, which may contribute to increased thrombotic events associated with *S. aureus* sepsis [11].

2.3.3. Respiratory chain of *Staphylococcus aureus*

Staphylococcus aureus is a facultative anaerobic bacterium able to perform anaerobic and aerobic respiration. Under aerobic conditions *S. aureus* uses oxygen as the final electron acceptor, while under anaerobic conditions this bacterium may use nitrate as electron acceptor. Furthermore, *S. aureus* may also perform fermentation. *S. aureus* uses the glycolytic pathway to metabolize glucose and can also use the citric acid cycle and catabolism of amino acids to obtain energy [12] . These variable metabolic capacities allow *S. aureus* to adapt to different conditions, including host environments when acting as a pathogen. However and surprisingly the respiratory chain of *S. aureus* is quite simple.

The respiratory chain *of S. aureus* is constituted by different quinone reductases, such as Malate: quinone oxidoreductase (MQO); Pyruvate:quinone oxidoreductase (PQO); Succinate:quinone oxidoreductase (SDH); Glycerol-3-phosphate:quinone oxidoreductase (G3PQO); Sulfide:quinone oxidoreductase (SQR); Dihydroorotate:quinone oxidoreductase (DHOQO). Type 2 NADH:quinone oxidoreductase (Ndh-2), an alternative enzyme to Complex I, is also present in respiratory chain since in the genome of *S. aureus* the genes encoding for Complex I are not present [13].

Besides quinone reductases, the so-called MpsABC seems to represent an important functional system of the respiratory chain of *S. aureus* that acts as an electrogenic unit responsible for the generation of membrane potential [13].

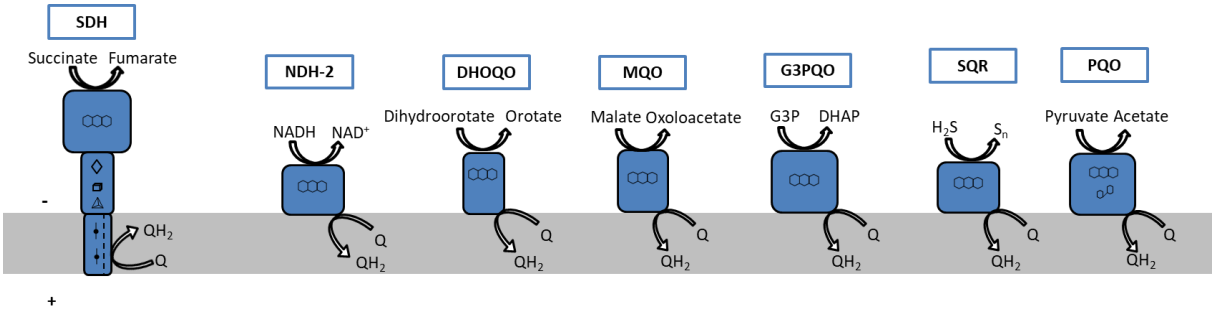

Figure 2.1- Schematic representation of quinone reductases from *Staphylococcus aureus* respiratory chain. FAD is represented by ⬡⬡⬡, TPP is represented by ⬡⬡, the [2Fe-2S] cluster is represented by ◇, the [4Fe-4S] cluster is represented by ▣, [3 Fe- 4S] cluster is represented by ⚠ and the heme is represented by ⚲. (+ and – indicate the positive and negative sides of the transmembrane difference in electrochemical potential, respectively) Adapted from Marreiros *et al*, 2016

2.4. Monotopic membrane proteins

Membrane proteins can be classified into two broad categories, integral and peripheral proteins, based on the nature of the membrane-protein interactions.

Integral membrane proteins, also called intrinsic proteins, have one or more segments that are embedded in the phospholipid bilayer. Most integral proteins contain amino acid residues with hydrophobic side chains that interact with fatty acyl groups of the membrane phospholipids, thus anchoring the protein to the membrane. By contrast, peripheral membrane proteins, or extrinsic proteins, do not interact with the hydrophobic core of the phospholipid bilayer, instead they are usually bound to the membrane indirectly by interactions with integral membrane proteins or directly by interactions with lipid polar head groups. In the latter case these are also called monotopic membrane proteins because they only interact with one leaflet of the lipid bilayer and do not possess transmembrane spanning segments [14].

In this work we selected to study DHOQO, G3PQO and PQO, which have been described as monotopic enzymes, localized and attached to one side of the surface of the lipid bilayer through electrostatic and hydrophobic interactions. They are identified with important physiological functions, as drug target in different type of organisms, but until now only few of them have been studied. In the case of these three quinone reductases from *Staphylococcus aureus* under study not much information exist in the literature, and because of that this thesis proposed to carry out and extensive biochemically and cellular characterization of these proteins.

The selected enzymes are flavoproteins and catalyze the two electrons oxidation of their respective electron donors to the reduction of menaquinone. The presence of the FAD or FMN as a prosthetic group attributes them a UV-Visible spectrum of flavoproteins with maxima at 375 nm and 450 nm, resulting in a characteristic yellow color of the protein samples.

2.4.1. Dihydroorotate:quinone oxidoreductase

Dihydroorotate:quinone oxidoreductase (DHOQO, EC:1.3.5.2) is a flavin mononucleotide (FMN) containing enzyme, which catalyzes the oxidation of dihydroorotate to orotate and the reduction of the quinone to quinol. This enzymatic reaction corresponds to the fourth and only redox step in the pyrimidine biosynthetic pathway, which is present both in eukaryotes and prokaryotes. DHOQO from *Staphylococcus aureus* is a monotopic membrane enzyme, encoded by the gene *pyrD* and has a molecular mass of 39 kDa. This protein is widely spread through the three domains of life [15] [16] [17]. The crystallographic structures of the *Escherichia coli* and *Homo sapiens* have been determined.

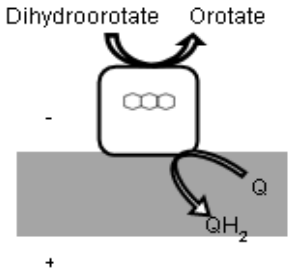

Figure 2.2- Schematic representation of Dihydroorotate:quinone oxidoreductase, a monotopic protein, that catalyzes the oxidation of Dihydroorotate to Orotate and the reduction of quinone to quinol. FMN is represented by three rings. (+ and – indicate the positive and negative sides of the transmembrane difference in electrochemical potential, respectively) Adapted from Marreiros *et al*,2016.

2.4.2. Glycerol-3-phosphate:quinone oxidoreductase

Two different G3PQO are encoded in *E. coli*, depending of the presence or absence of oxygen. The presence of GlpD (the aerobic form) is observed in the three domains, whereas genes coding for GlpABC (anaerobic expressed form) are present in 9% bacterial species, in 17% of the archaeal species and are not observed in Eukarya [18] [19].

Glycerol-3-phosphate: quinone oxidoreductase from *Staphylococcus aureus* (G3PQO, EC:1.1.5.3) is a monotopic membrane protein encoded by the gene *glpD* and presents the molecular mass of 62 kDa. This enzyme contains FAD as cofactor and catalyzes the oxidation of glycerol-3-phosphate (G3P) to dihydroxyacetone phosphate (DHAP) with reduction of quinone. GlpD has been characterized in organisms from all domains of life such as the bacterium *E. coli* [20], the archae on *Haloferax volcanii* [21] and the eukaryote *Wistar rat* [22].

Recently, overexpression of GlpD was associated with the increased tolerance to different antibiotics by persisters (subpopulations) of a bacterial culture of *E. coli* [23].

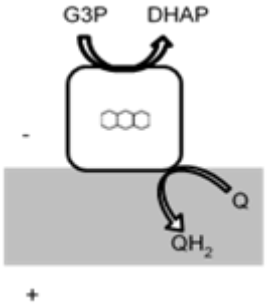

Figure 2.3- Schematic representation of Glycerol-3-phosphate quinone oxidoreductase, a monotopic protein, that catalyzes the oxidation of Glycerol-3-phosphate to Dihydroxyacetone phosphate and the reduction of quinone to quinol. FAD is represented by three rings. (+ and – indicate the positive and negative sides of the transmembrane difference in electrochemical potential, respectively) Adapted from Marreiros *et al*,2016

2.4.3. Pyruvate:quinone oxidoreductase

Pyruvate:quinone oxidoreductase (PQO, EC 1.2.5.1.) catalyzes the oxidative decarboxylation of pyruvate to acetate and CO_2 with transfer of electrons to quinone. The PQO contains FAD, thiamine pyrophosphate (TPP) and Mg^{2+} as cofactors. In *S. aureus*, this protein is encoded by the gene *CidC* and has a molecular mass of 63 kDa. Recent studies revealed an important role for the *S. aureus* PQO enzyme in cell death during the stationary phase and in biofilm development. The gene that codes PQO is only present in Bacteria and Archaea [24] [25] and this enzyme has been only described in bacteria such as *C. glutamicum* [25] and *E. coli* [26].

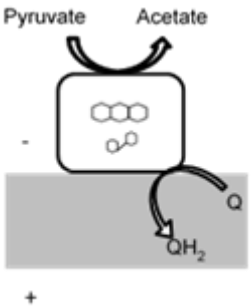

Figure 2.4- Schematic representation of Pyruvate:quinone oxidoreductase, a monotopic protein, that catalyzes the oxidative decarboxylation of pyruvate to acetate and CO_2 reducing the quinone to quinol. FAD is represented by three rings, and TPP is represented by two rings. (+ and – indicate the positive and negative sides of the transmembrane difference in electrochemical potential, respectively) Adapted from Marreiros *et al*,2016

3. Materials and Methods

3.1. Protein expression and purification

At the beginning of this project, G3PQO and PQO were already purified according to the same protocol here on described. The expression and purification of DHOQO, by contrast, was performed and optimized as described below.

The plasmid pET-28a (+) (Novagen) carrying the gene coding for DHOQO from *S. aureus* NCTC8325 and a poly-histidine tail in N-terminal position was already available. The gene product corresponds to a 354 amino acid residues protein with a theoretical molecular mass of 39 kDa. *E. coli Rosetta 2 (DE3) pLysS* cells were transformed with this plasmid using a heat shock protocol [27]. The cells were grown in Terrific Broth (TB) medium supplemented with 100 µg/mL of kanamycin and 34 µg/ mL of chloramphenicol at 37 °C and 180 rpm. The plasmid contains a resistance cassette to kanamycin, whereas *E. coli Rosetta 2 (DE3) pLysS* cells are resistant to chloramphenicol. Protein expression was induced by the addition of 1 mM IPTG (isopropyl-d-1-thiogalactopyrano) when cells reached an optical density, OD_{600}, of 0.6. Cells were harvested after an overnight growth by centrifugation at 8,655×g for 10 minutes at 4 °C and stored at -20 °C until further use.

To initiate the purification protocol, cells were thawed and resuspended in 50 mM K_2HPO_4/KH_2PO_4 pH 7.0, 250 mM NaCl, 10 % glycerol buffer, containing one complete protease-inhibitor cocktail tablet (Roche) and Lysozyme (Sigma). Cells were disrupted using the Mynilysis equipment (Bertin Technologies) with three cycles of 45 seconds, at maximum speed. Disrupted cells were separated from non-disrupted ones, and from the glass beads, by centrifugation at 4,100 ×g for 20 min at 4°C. The resulting supernatant was ultracentrifuged at 20,4709 ×g for 2 h at 4 °C. The membrane pellet (membrane fraction 1) was resuspended with a Potter-Elvehjem homogenizer in 50 mM K_2HPO_4/KH_2PO_4 pH 7.0, 2 M NaCl, 10 % glycerol buffer and incubated overnight under agitation at 4 °C. The high ionic strength was used in order to dissociate electrostatically attached membrane proteins. Membrane fraction 1 was again ultracentrifuged at 20,4709 ×g for 1 hour at 4 °C and soluble fraction 2 and membrane fraction 2 were obtained. The NaCl concentration of the supernatant (soluble fraction 2) was decreased to approximately 500 mM by dilution with buffer 50 mM K_2HPO_4/KH_2PO_4 pH 7.0, 10 % glycerol. Then, soluble fraction 1 and soluble fraction 2 were separately injected in an His-Trap IMAC 5 mL column (Thermo Fisher) operated in a AKTA Prime Plus system (GE Healthcare). The column was equilibrated with Buffer A, 50 mM K_2HPO_4/KH_2PO_4 pH 7.0, 250 mM NaCl and the elution were performed using the Buffer B, 50 mM K_2HPO_4/KH_2PO_4 pH 7.0, 250 mM NaCl, 250 mM Histidines, 10 % glycerol. The samples were eluted using a gradient of buffer B between 0 and 100 % at 3 mL/min and the elution of the sample was monitored by the change in absorbance at 280 nm.

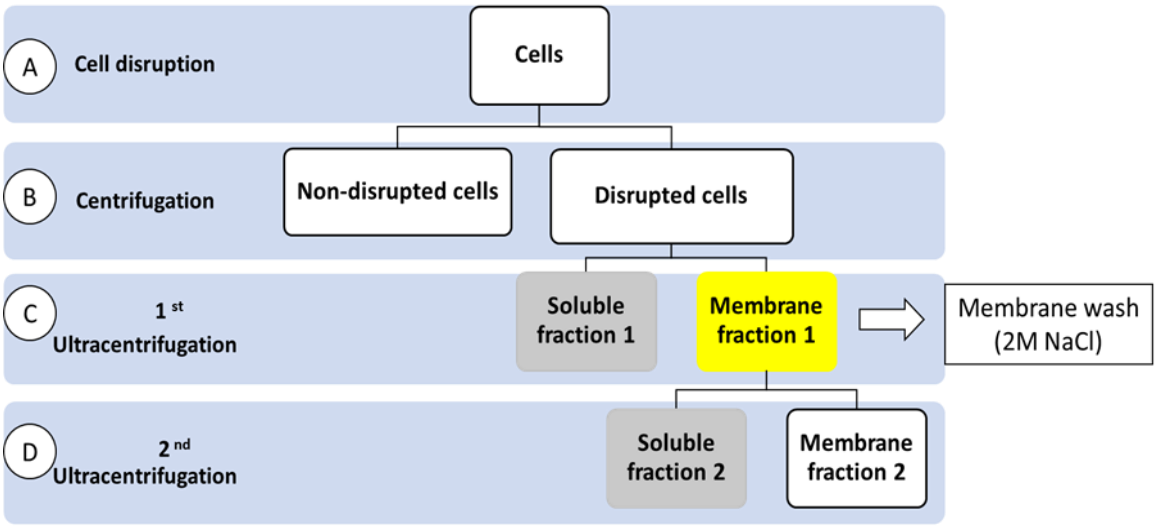

Figure 3.1- Schematic representation of the purification process. A- The cells were disrupted by mechanical lysis. B- The separation of the disrupted cells and the non-disrupted cells was obtained by centrifugation. C- The separation of the soluble fraction 1 and membrane fraction 1 of the resulted supernatant was obtained by ultracentrifugation. After the membrane fraction 1 was washed using a buffer containing a high ionic strength. D- The separation of the soluble fraction 2 and the membrane fraction 2 was done by ultracentrifugation. The two soluble fractions obtained were injected in the IMAC His-Trap HP column 5 mL.

The fractions that presented a characteristic flavoprotein spectrum were concentrated with an Amicon system (30 000 MWCO) by successive centrifugations.

The concentration of total protein was determined by the Pierce BCA (Bicinchoninic Acid) protein assay kit [28] and the concentration of the flavoprotein was obtained using the FMN extinction coefficient of 12.2 M^{-1} cm^{-1} [29].

3.2. Biochemical Characterization

The biochemical characterization of the proteins aimed first, to evaluate the quality and purity of the samples containing the protein of interest, by determining its concentration and overall purity by SDS-PAGE.

The biochemical characterization also focused on the UV-Visible spectra of the target proteins, on their melting temperature, on cofactor identification, on their oligomerization state and on assessing the enzymatic activity of the same three proteins, determining their kinetics parameters (V_{max} and K_M).

Lastly, we performed fluorescence spectroscopy studies, targeting the protein substrate interaction, allowing to study the affinity and overall binding of different enzyme ligands.

3.2.1. SDS- PAGE

Protein purity was evaluated by sodium sulphate-polyacrylamide gel electrophoresis (SDS-PAGE) using a mini-PROTEAN Electrophoresis System (BiORAD).

The samples were diluted in 5 µL of loading buffer (Tris-HCl 50 mM pH 8, SDS, Bromophenol Blue, Glycerol, β-mercaptethanol and Urea) and incubated at 100 ºC for 5 minutes. The resulted mixture was injected in 4 % and 12.5 % acrylamide stacking and resolving gel respectively. PeqGOLD protein-Marker iv was used as protein mass marker ranging from 10 to 170 kDa. Protein bands were revealed using Blue Coomassie Stainer (0.1 %) and distaining solution.

3.2.2. Oligomerization state identification

In order to estimate the oligomerization state of the proteins a NativePAGE Novex Bis-Tris (Thermo Fisher) was performed using a mini-PROTEAN Electrophoresis System (BiORAD).

The protein samples were prepared to a final volume of 10 µL 0.5 µg of each protein was mixed with NativePAGE sample Buffer (4×) and NativePAGE Coomassie G-250 5 %. The samples were injected in 4-16 % gradient acrylamide gels and were ran at 150 V for 120 minutes. The High Molecular Weight Calibration (HMW) kit (Amersham Biosciences) was used as protein mass marker ranging from 66 to 669 kDa. The anode buffer used was 50 mM Bis-Tris 50 mM Tricine pH 6.8 and the cathode buffer was 50 mM Tricine, 15 mM Bis-Tris pH 6.8, and 0.5 % Brilliant Blue G-250. Protein bands were stained with Blue Coomassie Stainer (0.1%) and distaining solution

3.2.3. Protein reduction and reoxidation

Protein reduction and reoxidation using UV–Visible absorption spectroscopy assays were performed on a Shimadzu UV-1900 spectrophotometer equipped with a Peltier temperature controller and a stirring device. To ensure O_2-free conditions, in all assays an oxygen scavenging system was used, composed of 5 mM glucose (Roth), 4 U/mL glucose oxidase (Sigma Aldrich) and 130 U/mL catalase (Sigma Aldrich). Reduction of 6 µM of the DHOQO in 100 mM KH_2PO_4/K_2HPO_4 buffer pH 7.0, 250 mM NaCl was achieved by addition of 6 µM of Dihydroorotate (electron donor). Reoxidation was observed by addition of the same concentration of DMN (2,3-Dimethyl-1,4-naphthoquinone) to maintain a 1:1 ratio between substrates.

3.2.4. Cofactor identification

The flavin prosthetic group was identified by High Performance Liquid Chromatography (HPLC) using a reverse chromatography column. The protein was denatured by incubation at 100 °C for 10 min (until the solution was turbid). The separation of the denaturated protein and cofactors was performed by centrifugation at 16,200 ×g for 15 minutes. After filtration with a 0.2 µm pore syringe filter (VWR), 30 µL of the supernatant was injected in a Luna C18 column 3 µm (150 × 4.60 mm; Phenomenex) operated in a HPLC system (Dionex Ultimate 3000) that was coupled to a spectrophotometer. Each chromatography lasted approximately 25 minutes, during which eluted samples were followed by UV-Vis spectroscopy. The column was equilibrated with buffer A, 5 mM ammonium sulfate. The elution was performed using the buffer B, 5 % methanol. The sample was eluted in the same buffer with an isocratic gradient from 10 to 80 % of methanol at 1 mL^{-1} min^{-1}. Solutions of 100 µM of FAD, FMN and TPP were used as standards.

3.2.5. Thermal denaturation

In order to study the thermal stability of the interest proteins, thermal denaturation assays were performed in a Varian Cary Eclipse spectrofluorometer equipped with a Peltier temperature controller. Samples were excited at 450 nm and fluorescence emission was followed at 530 nm, at increasing temperatures with a rate of 0.5 °C/min between 25 and 90 °C. Data was recorded with 1 °C intervals and an acquisition time of 0.1 min. Two independent assays were performed using 2 µM protein in 100 mM KH_2PO_4/K_2HPO_4 buffer pH 7.0, 250 mM NaCl. Melting temperatures were calculated by fitting a Boltzmann equation to the experimental points using the OriginPro8 software.

3.2.6. Protein Substrate interaction

Protein substrate interaction was monitored by fluorescence spectroscopy studies performed on a Fluorolog-3 (HORIBA Jobin Yvon) spectrofluorometer. The initial reaction mixture contained 2 µM of

protein in 100 mM K_2HPO_4/KH_2PO_4 pH 7.0, 250 mM NaCl. Conformational changes in the protein due to interactions with DMN (2,3- Dimethyl-1,4-naphthoquinone), DUR (Duroquinone), HQNO (2-n-Heptyl-4-hydroxyquinoline N-oxide) and the electrons donors dihydroorotate, G3P and pyruvate were investigated. Three independent titrations were performed with substrates ranging from 0 to 250 µM. Tryptophan and flavin fluorescence emission spectra were recorded at 25 °C with excitation wavelength of 295 nm and 450 nm, respectively. The reduction in emission at 351 nm, with excitation at 295 nm, (ΔF) was normalized and represented versus the substrate concentration. In order to determine the dissociation constants (K_D), the obtained titration data was fitted using the Monod-Wyman-Changeux (MWC) model equation, , $\Delta F = \Delta F^{max} \times \frac{\frac{[S]}{K_S}\left(1+\frac{[S]}{K_S}\right)}{L+\left(1+\frac{[S]}{K_S}\right)^2}$

3.2.7. Catalytic activity and pH profile

The enzymatic activity of DHOQO was tested at different pH values to determine the most favorable pH value for activity. Experiments were performed in duplicates, at 37 °C and following the change in absorbance at 270 nm (corresponding to DMN reduction). The concentration of the substrates was kept constant at all the across different pH values tested, with 150 µM of DMN, as electron acceptor, and 150 µM of Dihydroorotate, as electron donor. pH values between 5.5 and 9 were tested using 50 mM MES, 50 mM Bis-Tris Propane, 250 mM NaCl buffer. The concentration of protein used was 0.125 µM.

3.2.8. Steady state kinetics studies

The enzyme kinetics measurements of DHOQO were performed at 37 °C on a Shimadzu UV-1900 spectrophotometer monitoring the change in the absorbance at 270 nm (extinction coefficient of 17545 $M^{-1}\,cm^{-1}$). Enzymatic activities were determined using DMN as electron acceptor, and with Dihydroorotate as the electron donor.

In one case (to determine DMN kinetic parameters), 125 µM DMN was kept constant and the titration of dihydroorotate was performed in range of 0 to 300 µM. To determine dihydroorotate kinetic parameters 150 µM dihydroorotate was used and the titration of DMN was done in range of 0 to 125 µM. Triplicates for each substrate concentration were performed, in both DMN and dihydroorotate titrations. To obtain the kinetic parameters the data was fitted using the Michaelis–Menten equation $v = \frac{Vmax\,[S]}{Km+[S]}$

The interference of the inhibitor HQNO (2-n-Heptyl-4-hydroxyquinoline N-oxide, $C_{16}H_{21}NO_2$) in the activity of the protein was tested. The reaction mixture contained 0.125 µM protein, 150 µM of electron donor and 125 µM of DMN in 50 mM MES 50 mM Bis- Tris propane, 250 mM NaCl buffer pH 7.5. Independent titrations were performed with HQNO in the range of 1 to 100 µM. The K_i constant were obtained fitted the data points using equation $v_0^i = v_0^{max}\frac{\left(1+\beta\frac{[I]}{Ki}\right)}{\left(1+\frac{[I]}{Ki}\right)}$

3.3. Cellular characterization

The main goal of this part of the project was to understand the influence of three respiratory chain proteins on the metabolism of the *Staphylococcus aureus*. For that knockouts mutants of DHOQO, G3PQO and PQO were built.

The process of the construction of the knockouts mutants involved 5 main steps: 1) amplification of the up and down fragments of the respected gene by PCR; 2) join these fragments using overlapping PCR; 3) cloning the product of the overlapping PCR into pMAD vector; 4) electroporation into *S.aureus* RN4220; 5) transduction (using the phage 88α) *S. aureus* MW2.

Routine DNA procedures such as DNA digestion with restriction enzymes, DNA ligations and agarose gel electrophoresis, transformations and transduction process were performed.

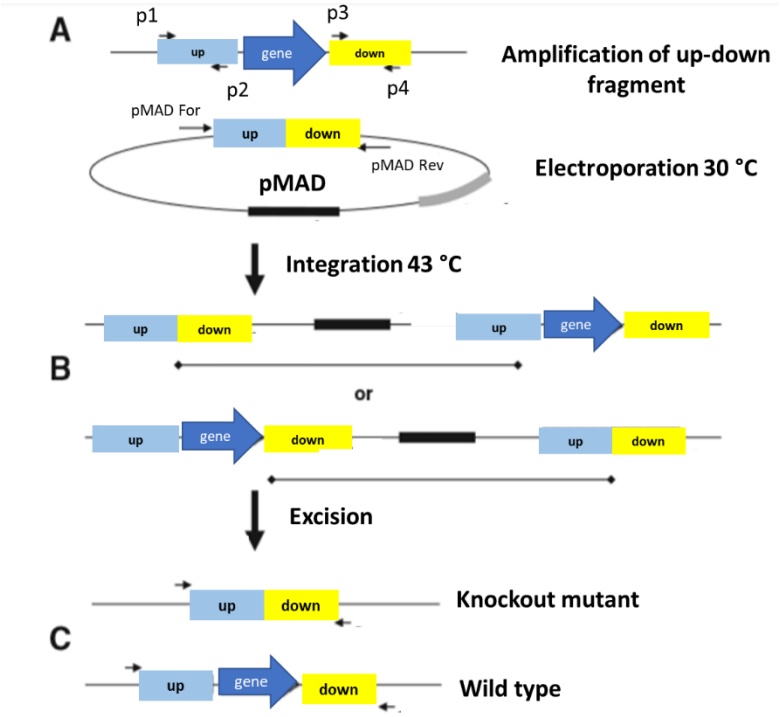

Figure 3.2- Schematic representation of the different steps of the construction of the DHOQO, G3PQO and PQO knockouts mutants. A- gene encoding for the DHOQO, G3PQO and PQO proteins, flanked by two homologous regions, upstream and downstream regions. The first step is the amplification of these two regions and the overlap fragment. The resulted fragment was cloned into pMAD vector. The construct was then electroporated into S. aureus RN4220. B- Integration of the plasmid into the genome by homologous recombination achieved at 43ºC, a non-permissive temperature for the plasmid replication, while maintaining selection for the erythromycin and X-gal. The first recombination event could occur in upstream or downstream region. C- The excision of the plasmid region in chromosome by double-crossover event in the opposite side of the integration event leads to the protein gene deletion, while in the same side leads to regeneration of the wild-type. Adapted from Kato *et al.*

3.3.1. Construction of knockouts mutants of DHOQO, G3PQO and PQO

Table 3.1- Oligonucleotide primers used in this study.

Primer name	Nucleotide sequence (5´-3´)
P1-DHOQO KO	CGCCCGGGTCACTTTTATTGTAACTCAACCTT
P2-DHOQO KO	ACTATGTTGGAGAGTATGCTCCTATTTCATTATA
P3-DHOQO KO	TACTCTCCAACATAGTCAAATAATACTTTAA
P4-DHOQO KO	CCACGCGTATGACAAGGTGTTGAAGAAATTAAT
P1-G3PQO KO	CGCCCGGGTTAGAGATAAGACAGGATTACTT
P2-G3PQO KO	TATGATTGTACAAATTAATCCAAAACGCCTCCTAAA
P3-G3PQO KO	TTAATTTGTACAATCATAAACTGGTG
P4-G3PQO KO	CGGTCGACTCATCAGGATTCAAGATATCAATT
P1-PQO KO	GCCCCGGGAAGCACTCATTATTTAAGGC
P2-PQO KO	TATTACTAATAGCCTCCCTTTCTG
P3-PQO KO	GAGGCTATTAGTAATATTTAGATCAAATTCCACC
P4-PQO KO	CCGGATCCTCCTGCTGATAACATTAAAC
pMAD Forward	CTCCTCCGTAACAAATTGAGG
pMAD Reverse	CGTCATCTACCTGCCTGGAC

3.3.1.1. Amplification of up-down fragment

The knockout mutants for DHOQO, G3PQO and PQO were constructed using the purified genomic DNA from *Staphylococcus aureus* USA 300 strain and the vector pMAD.

Two PCR fragments, corresponding to the 1300 bp upstream and 1300 bp downstream regions (approximately) of the gene coding for the DHOQO, G3PQO and PQO were amplified from chromosomal DNA of strain USA 300 using Phusion high-fidelity DNA polymerase (Finnzymes) and primer pairs P1/ P2 and P3/ P4, supplied by Eurofins. Then, the two fragments were joined by overlapping PCR using primers P1 and P4. The correct size of each fragment was confirmed by electrophoresis on a 1 % agarose gel, followed by clean-up of the PCR products using the Clean-up Wizard Kit (Promega).

3.3.1.2. Digestion of plasmid and inserts

The resulting inserts and pMAD vector were digested with appropriate High-fidelity restriction enzymes (NEB) (0.2-1 μg DNA, 1X restriction buffer and water to 50 μL for 2 hours 30 minutes). By heating the samples at 70 °C for 10 min the digest reaction was inactivated. The samples clean-up was done using the Clean-up Wizard Kit (Promega).

3.3.1.3. Competent cells of *E. coli* DC10B

E. coli DC10B competent cells were grown until OD_{600} = 0.5 and harvested by centrifugation 2,400 ×g for 5 minutes at room temperature. Cells were resuspended in 750 µL of cold and sterilized 100 mM $CaCl_2$ and incubated on ice for 1 hour. Centrifugation at 2,400 ×g for 5 minutes at room temperature allowed to resuspend the resulting in 100 µL of 100 mM $CaCl_2$ followed by another incubation of 1 hour. Cells were stored at -80 °C until further use.

3.3.1.4. Ligation of digested plasmid and insert

The ligation of the digested pMAD plasmid and insert of interest was done with a proportion 6:3 (insert: plasmid) using a T4 Ligase (Promega) and incubated either for 3 hours at room temperature, or alternatively for 16 hours at 4 ºC. Next, *E. coli* DC10B competent cells were transformed with 5 µL of the ligation mix and kept on ice for 30 min. Foreign DNA was introduced using a heat shock method (45 seconds at 42 °C). Cells were mixed with 1 mL LB medium and incubated at 37 °C for 1.5 hours and then spread on LA plates with 100 µg/mL ampicillin. Colony screening of the obtained colonies was performed by PCR colony reaction with Taq Polymerase (VWR) using the pair of the primers pMAD forward and pMAD reverse. The cloned product was extracted from positives grown colonies and sent to be sequenced (Eurofins).

3.3.1.5. Competent cells of *S. aureus* RN4220

Cells of *S. aureus* RN4220 were grown to OD_{600} = 0.4 and centrifugated at 6,200 ×g for 15 minutes at 4 ºC. Cells were washed with equal volume of culture of cold filter and sterilized 0.5 M sucrose, and centrifugated again, and resuspended in half of the volume of 0.5 M sucrose. Cells were then incubated on ice for 15 minutes and resuspended in 300 µL of 0.5 M sucrose and stored at -80 °C.

3.3.1.6. Electroporation

Electroporation was performed by mixing 50 µL of competent cells of *S. aureus* RN4220 with 5 µL of the replicative plasmid pMAD extracted from *E. coli* DC10B in a 2.0 mm electroporation cuvette (Bio-Rad) and subjected to an electroporation pulse in a Gene Pulser Xcell equipment (Bio-Rad) set to 2.5 kV, 25 µF and 100 Ω. Cells were incubated 5 minutes on ice and resuspended in 1 mL of Tryptic Soy Broth (TSB) medium. Cells were incubated for 1 hour at 37 °C and plated on Tryptic Soy Agar (TSA) supplemented with 10 µg/mL erythromycin (Ery) and 100 µg/mL X-gal (5-Bromo-4-chloro-3-indolyl β-D-galactopyranoside). The plates were incubated at 30 °C for 48 hours.

3.3.1.7. Transduction with phage 88 α

For the transduction lysates, *Staphylococcus aureus* RN4220 (donor strain) were grown in Tryptic Soy Agar (Difco) overnight at 37 °C in order to have rich confluent growth. Cells were resuspended in 1 mL of TSB with 5 mM of $CaCl_2$.

Phage 88 α lysate was diluted in 1 mL of phage buffer (1mM $MgSO_4$, 4 mM $CaCl_2$, 50 mM Tris-HCl pH 7.8, 5.9 g/L NaCl and 1 g/L gelatin). The cell suspension, 10 µL, was mixed with 10 µL of each of the phage dilutions and 3 mL of phage top agar medium, supplemented with 5 mM of $CaCl_2$, pre-warmed for one hour at 45 °C. The mixture was poured onto phage bottom agar with 5 mM of $CaCl_2$ and incubated overnight at 30 °C.

Following the transduction, 3-4 mL of phage buffer was added to plates showing confluent lysis. Plates were incubated at 4 ºC for 1 hour. The phage top agar and the phage buffer were then collected into a centrifuge tube and vortexed in order to disrupt the phage bottom agar. The tubes were incubated for 1 hour inverted at 4 °C. The agar was centrifugated at 1,200× g for 15 minutes at 4 °C to sediment top agar. The supernatant was collected and filtered through a 0.45 µm sterile filter. The recipient strains (*S. aureus* MW2) were grown overnight in TSA at 37 °C in order to have rich confluent growth.

Cells (two full 10 µL loops) were resuspended in 1 mL TSB with 5mM $CaCl_2$. 100 µL of cell suspension was added to 1 µL of the phage lysate and 100 µL of phage buffer. A control tube without phage lysate was prepared. The mixture was incubated for 20 minutes at 37 °C under agitation and was mixed with 3 mL of 0.3 GL top agar at 45 °C. The final mixture was then poured onto plates made with 10 mL of 0.3 GL bottom agar with 30 µg/mL of Erythromycin and 20 mL of 0.3 GL bottom agar without antibiotic. The plates were incubated at 30 ºC overnight.

3.3.1.8. Integration and Excision of pMAD

One single colony were grown in 5 mL of TSB supplemented with 10 µg/mL Ery at 30 ºC overnight. The overnight culture was diluted 1:1000 into 5 mL of fresh TSB medium supplemented with 10 µg/mL Ery and was incubated at 30 ºC for 8 hours. After 8 hours grown, were done a dilution (1:1000) in the same medium and incubated overnight at 43 ºC, to occurs the integration process.

Dilutions of the overnight culture (10^{-4}, 10^{-5}, 10^{-6}) were performed and were plated in TSA supplemented with 10 µg/mL Ery and 100 µg/mL X-Gal plates and incubated at 43 ºC overnight.

The blue colonies were re-plated into TSA supplemented with 10 µg/mL Ery and 100 µg/mL X-Gal and incubated at 43 ºC overnight, in order to obtain a confluent growth. To ensure if the colonies were positives ones, were performed the extraction of genomic DNA from each of the clones and were done the PCR colony.

The positives colonies were inoculated in TSB medium at 30 ºC overnight. The dilution of the overnight culture was done (1:500) in fresh TSB and incubated at 30 ºC for 8 hours. After the 8 hours growth, successive dilutions were done (10^{-4}, 10^{-5}, 10^{-6}) and were plated in TSA supplemented with 100 µg/mL X-Gal. The plates were incubated at 43 ºC overnight. The white colonies were re-plate into TSA+ 100

µg/mL X-Gal plates and were incubated at 43 ºC overnight and were performed the colony screening. The positives colonies were confirmed by sequencing (Eurofins).

3.3.2. Cellular Studies

3.3.2.1. Cell Growth

Staphylococcus aureus MW2 strains (WT and ΔDHOQO) were grown in TSA medium plates and incubated at 37 ºC overnight. Inoculums of one single colony were done, in triplicates, and grown for 16 hours under aerobic conditions in TSB medium at 37 ºC and 180 rpm.

S. aureus growths were performed in TSB medium. Two different conditions were monitored during the growth, the optical density at 600 nm ($OD_{600\ nm}$) (Ultrospec 10 cell density meter, Armersham Biosciences) and the pH (pH meter GLP 22, Crison Instruments, SA), measured each 1.5 hours. 50 mL of cellular culture were grown in aerobic condition in Erlenmeyer 250 mL (VWR) in an orbital shaker (INFORS HT) at 180 rpm at 37 ºC. Cultures were initiated with an initial $OD_{600\ nm}$ of 0.05.

The handling of *S. aureus* was performed inside a laminar flow chamber (NinoSAFE Klass II 1200, nino labinterior) ensuring sterile conditions.

4. Results and Discussion

4.1. Expression of DHOQO from *Staphylococcus aureus*

At the beginning of this project G3PQO and PQO were already purified and under study, in contrast the expression and purification of DHOQO needed optimization. In order to study and biochemically characterize all these proteins, expression and purification experiments of DHOQO were initiated.

DHOQO was expressed using *E. coli* Rosetta cells grown at 37 ºC and 180 rpm, in TB medium supplemented with 100 µg/mL of Kanamycin and 34 µg/mL of Chloramphenicol. 1mM of IPTG was added to the cells culture at OD_{600} of 0.6.

When optimizing the expression conditions of DHOQO in *E. coli* Rosetta cells, the first tested condition was the time after induction. Four different times were assessed: 0h ("before induction"), 4h, 6h and overnight. Protein expression was monitored by SDS-PAGE (shown below).

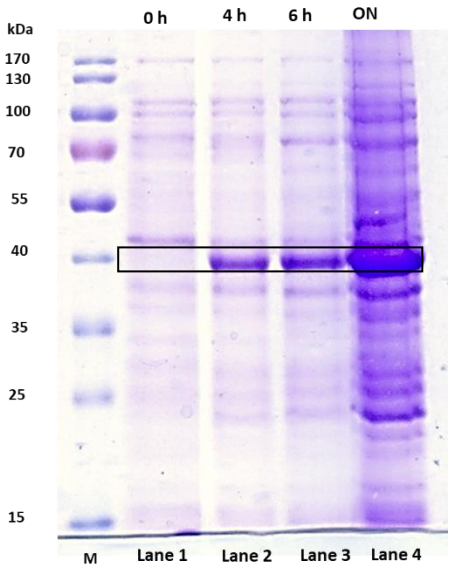

Figure 4.1- SDS-PAGE gel showing the DHOQO expression (highlighted in black). SDS-PAGE stacking gel 4 % and Resolving Gel 12.5 %.; Lane 1- protein expression profile in *E. coli* Rosetta cells before IPTG addition (OD_{600}= 0.6), Lane 2- protein expression profile after 4 hours of induction, Lane 3- protein expression profile after 6 hours of induction, Lane 4- protein expression profile after an overnight growth; Theoretical molecular mass of DHOQO: 39 kDa. M-PeqGOLD protein-Marker iv was used as protein mass marker ranging from 10 to 170 kDa.

The SDS-PAGE gel shows the presence of one intense band in the 39 kDa region in lanes 2,3 and 4, which is not observed in lane 1, confirming the expression of the protein of interest. As the expression of DHOQO seemed be similar in the three conditions tested (since the amount of cells was the same in each gel lane), we decided to do choose the "overnight" condition, which would allow to obtain a higher cell mass per mL of growth when compared with the other conditions.

Other conditions that could influence protein expression and that can be tested in a similar assay as the one described above are: IPTG concentration, temperature, aeration of the cellular culture, cell strain, growth medium. The initial chosen conditions for the variables here mentioned were chosen by experience of the host laboratory and optimized protocols. We opted not to further test any of these conditions since the expression levels were considered to be good, but if this would not have been the case, we could perform more extensive expression tests.

Upon optimizing protein expression we were now in conditions to advance to cell growths and protein purification steps.

4.2. Purification of DHOQO

To harvest enough cell mass to start with the protein purification steps, *E. coli* Rosetta cells growths of 4 liters were performed. After the optimized overnight expression, cells were harvested and stored at -20 ºC until a total cell mass of 110 g was achieved. The growth yield was approximately 6 g of cells per liter of medium.

To initiate the purification process, cells (23 g of cells) were resuspended in 50 mM K_2HPO_4/KH_2PO_4 pH 7.0, 250 mM NaCl, 10 % glycerol buffer, before being disrupted using the Mynilysis Equipment. The disrupted cells and the non-disrupted ones (and the glass beads) were separated by centrifugation at 4,100× g for 20 min at 4 °C. Membrane and soluble fractions were separated by ultracentrifugation at 20,4709 ×g at 4 ºC.

The bacterial cell lysis can involve the use of different methods, such as the enzymatic and chemical lysis, mechanical disruption using the glass beads (Minilysis equipment) or using high pressure (French press). The mechanical lysis was the method used, since the hosting laboratory has the respective equipment and has obtained efficient cells disruption [30] [31].

Protein membrane extraction was achieved by washing the membranes with high ionic strength buffer (2 M NaCl). This procedure was possible to be implemented since the protein is attached to the membrane by electrostatic interactions, as is the case of the protein in study. The ions present in the used buffer will actively compete with the protein for membrane interaction, in this way forcing DHOQO out of the membrane and into the soluble fraction. An alternative was the use of detergents, but these are a far more expensive possibility, and may interfere with future assays.

The membrane fraction and soluble one resulted from the washing of the membranes with 2 M NaCl were separated again by ultracentrifugation and the presence of the protein was visible by the yellow color of the resulted supernatant. During the purification process the presence of the protein of interest was analyzed by SDS-PAGE and UV-vis spectroscopy. The results are shown in figure 4.2.

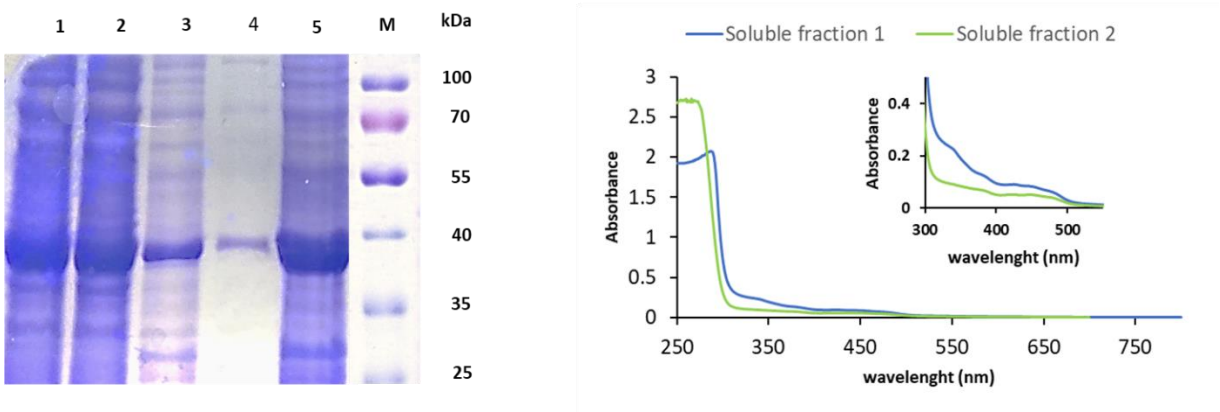

Figure 4.2- SDS-PAGE gel of the purification process of DHOQO. Lane 1- Disrupted cells, Lane 2- Soluble fraction 1, Lane 3- Membrane fraction 1 (2 M of NaCl), Lane 4- Soluble fraction 2, Lane 5- Membranes from second ultracentrifugation. Theoretical molecular mass of DHOQO: 39 kDa. PeqGOLD protein-Marker iv was used as protein mass marker ranging from 10 to 170 kDa. UV-visible spectra of the soluble fraction 1 (blue line) and soluble fraction 2 (green line) before the injection in the column, in 50 mM of 50 mM K_2HPO_4/KH_2PO_4 pH 7.0, 250 mM NaCl buffer.

Figure 4.2 shows the presence of the protein of interest in all steps of the purification process (presence of a strong band in the SDS-PAGE gel around the 39 kDa region). Observing the UV-visible spectra of the soluble fraction 1 and that of soluble fraction 2, before the injection in the IMAC column, the presence of characteristics flavoprotein peaks at 375 nm and at 450 nm were observed.

The two soluble fractions (two supernatant) obtained from the ultracentrifugations were injected in an affinity chromatography His-Trap HP IMAC column 5 mL, charged with the nickel ions (Ni^{2+}) and using a gradient of L-histidines as eluent. The DHOQO is expressed with a tail of six histidines inserted and so the Immobilized Metal ion Affinity Chromatography (IMAC) was chosen, since this tail is semi-specifically recognized by column resin [32].

Before the injection of the soluble fraction 2, the high ionic strength of the sample needed to be decreased, for that we subject this fraction to a dilution process with an equivalent buffer, with the only difference being the lack of salt. Dilution was performed until the ionic strength reached 500 mM of NaCl.

After injection, protein elution from the resin was done with buffer containing histidines that compete with the protein for the interaction with Ni^{2+}. The chromatographic process was monitored by following the absorbance at 280 nm. All eluted fractions were analyzed by UV-Visible spectroscopy.

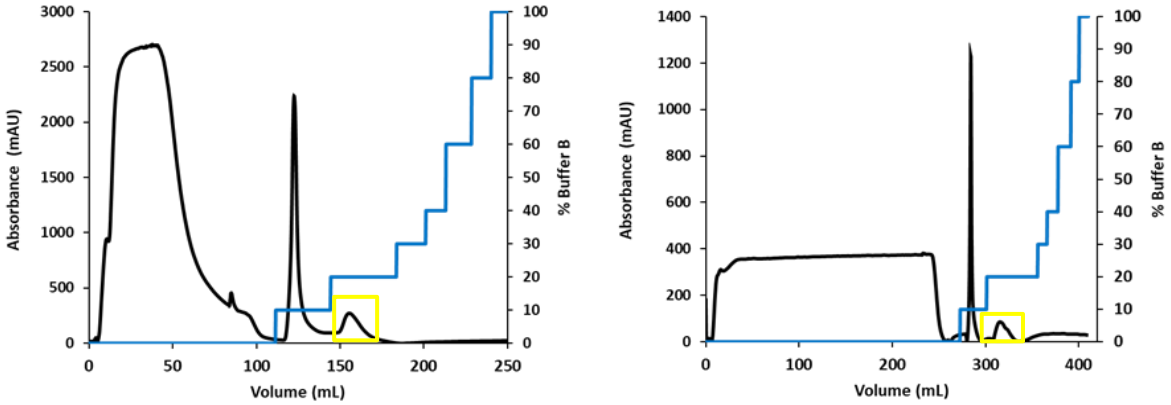

Figure 4.3- Chromatograms obtained in the purification process of DHOQO from Staphylococcus aureus. The chromatography was performed using a His-Trap HP 5 mL column with flux of 3 mL $^{-1}$ min $^{-1}$ and 0.8 MPa of the pression value. Buffer A was 50 mM K_2HPO_4/KH_2PO_4 pH 7.0, 250 mM NaCl and buffer B was 50 mM K_2HPO_4/KH_2PO_4 pH 7.0, 250 mM NaCl, 250 Mm of histidines. The elution was done using a gradient of the buffer B. Chromatogram A and B correspond a one injection of the soluble fraction 1 and the injection of the soluble fraction 2, respectively.

Analyzing the chromatograms represented below in figure 4.3 it was possible see that the protein was eluted at 20 % of buffer B (corresponding to a concentration of histidines of 50 mM). It was also observed the presence of the highest peak eluted at 10 % of buffer B, that does not correspond to the protein of interest, since this eluted fraction did not present the typical spectrum of a flavoprotein.

The fractions containing the DHOQO were those that presented the characteristic flavoprotein spectrum and a band in the SDS-PAGE gel on the region of 39 kDa. These fractions were separated according their ratio between the absorbance at 280 nm and 450 nm and were concentrated. This separation criterium resulted in four different fractions, for which the flavoprotein, and total protein concentration was determined. Additionally SDS-PAGE of this fractions was performed and is shown below in figure 4.4.

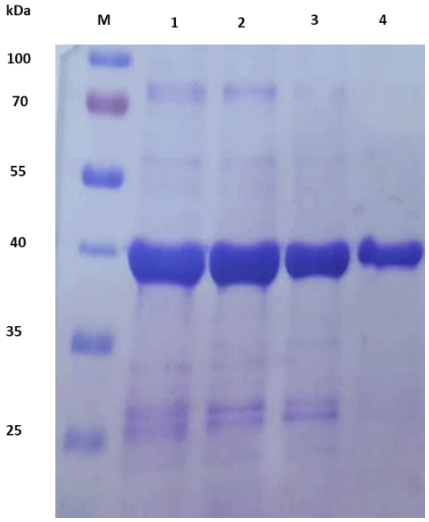

Figure 4.4- SDS-PAGE gel of the four fractions containing the DHOQO, resulted of the purification and after the concentration process. Lane 1- Fraction 1, Lane 2- Fraction 2, Lane 3- Fraction 3, Lane 4- Fraction 4; Theoretical molecular mass of DHOQO: 39 kDa. PeqGOLD protein-Marker iv was used as protein mass marker ranging from 10 to 170 kDa.

Figure 4.4 shows, the presence of a strong band in the expect region at 39 kDa and the presence of a small quantity of contaminating bands, indicating that protein was relatively pure in the four fractions.

The concentration of total protein was determined using the BCA protein quantification assay [28] and the respective protocol. The concentration of flavoprotein was calculated using the absorbance at 446 nm and the FMN extinction coefficient of 12.2 M^{-1} cm^{-1} [29], the results were summarized in figure 4.5.

Fraction	Concentration (mg/mL)	A280/A450
1	4.21	5.80
2	6.05	5.45
3	2.15	4.84
4	0.78	5.93

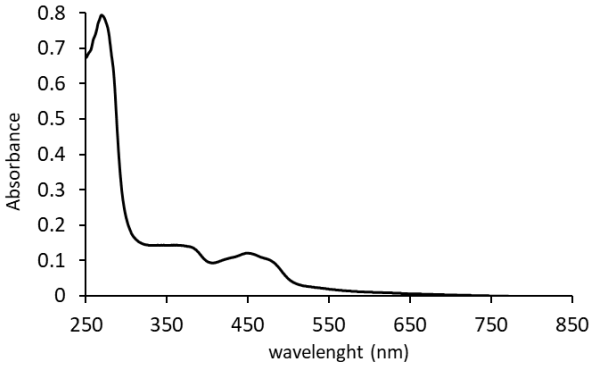

Figure 4.5- UV-visible spectrum of DHOQO fraction 1. The UV-visible spectrum presents the characteristic flavoprotein spectrum with maxima at 375 nm and 450 nm. Table total protein concentration obtained with the BCA quantification. The ratios between the absorbance at 280 nm and 450 nm are also presented.

All four fractions, after being concentrated, presented an absorption spectrum typical of a flavoprotein, exhibiting bands with maxima at 375 nm and 450 nm.

After the expression and purification process, the obtained DHOQO and the previously available preparations of G3PQO and PQO were biochemical and molecularly characterized.

4.3. Biochemical characterization

4.3.1. Thermal denaturation

To investigate the thermal stability of the proteins, also contributing to the biochemical and functional characterization of DHOQO, G3PQO and PQO thermal denaturation curves were performed. To do so, we measured the fluorescence emission intensity at 530 nm (excitation 450 nm, which corresponds the emission peak of FAD cofactor) between 25 and 90 ºC.

These assays provided the melting temperature of DHOQO, G3PQO and PQO, and are important to known the conditions in which the proteins are stable. The melting temperature can be interpreted as the temperature at which 50 % of the proteins in solution are denaturated and the other half maintained the folded conformation, this can be mathematically determined by the inflexion point in the sigmoid curve used to fit the obtained data.

Figure 4.6 presents the denaturation patterns of DHOQO and PQO, which show a sigmoid behavior, initiating at low emission intensities and increasing emission intensities with the increase in temperature. This increase in emission intensity can be explained by the enlargement of the exposure of the flavin cofactor caused by the progressive protein denaturation and loss of its conformation. The melting temperature was determined using *OriginPro 8 software,* fitting a Boltzmann function (sigmoid curve) to the obtained data. In the case of G3PQO the opposite situation is observed, where the denaturation pattern initiates at higher emission intensities and decreasing with the increases of the temperature. In this case the temperature produced an effect of hiding the flavin.

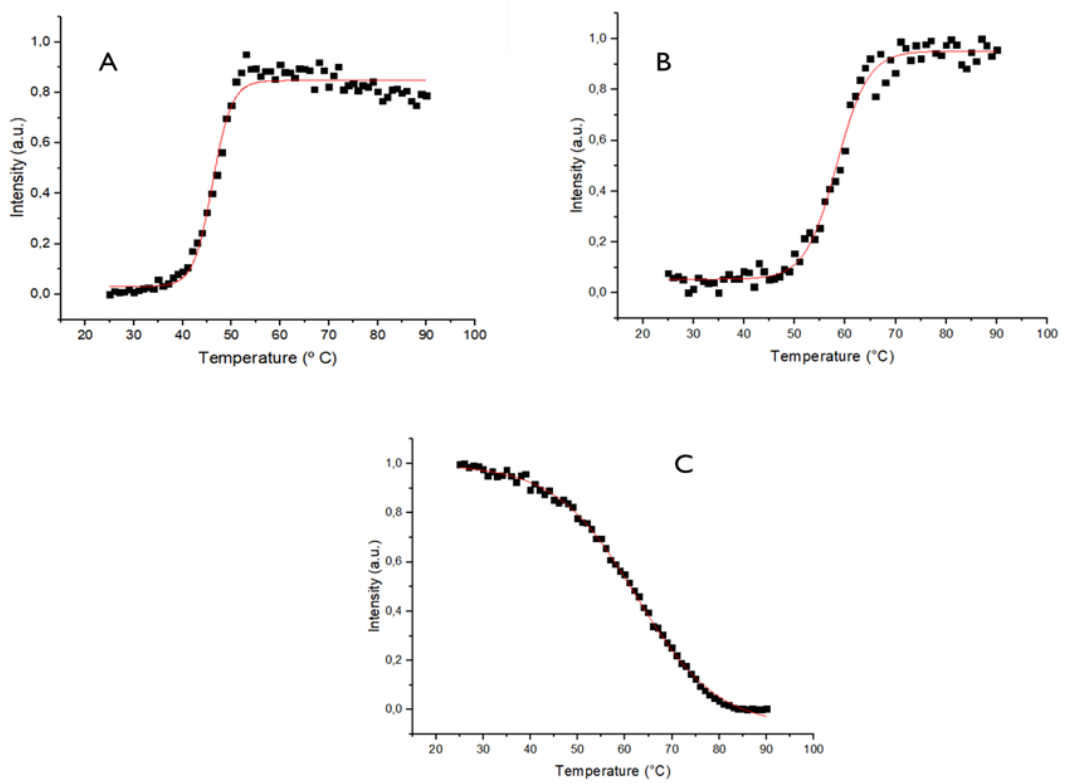

Figure 4.6- Thermal denaturation profile of DHOQO, G3PQO and PQO. In black dots is represented the fluorescence emission intensity at 530 nm in function of the temperature, between 25 and 90 ºC to each protein (2 µM). In dashed red lines is represented the sigmoid Boltzmann fit. A- DHOQO; B- PQO; C- G3PQO. Thermal denaturation assays were performed using a Peltier temperature controller with a rate of 0.5 °C/min and the data was recorded in intervals of 0.5 °C with acquisition time of 0.1 min.

The melting temperatures obtained for G3PQO and PQO were 62.3 ºC and 58.3 ºC respectively, meaning that the proteins present similar structural stabilities. For DHOQO the melting temperature was 46.1 º C, indicating that protein has a lower thermal stability.

4.3.2. Cofactor identification

The identification of the cofactors of the three quinone reductases in study was performed using a reverse-phase high- performance liquid chromatography (RP-HPLC), which involves the separation of molecules based on hydrophobicity [33].

The main goal of these assays was the identification of the prosthetic group of each protein, more specifically, differentiate if the cofactor of the proteins was a FAD or an FMN and determine whether PQO, besides the flavin, also had TPP as cofactor. For this, 3 standard containing solutions (one for each of the three cofactors), plus solutions containing extracted protein cofactors, were individually injected in the column and their retention times compared.

To prepare the samples for injection in the column, the solutions with each protein were subjected to thermal denaturation at 100 ºC, releasing its cofactors (supernatant). As the FAD, FMN and TPP are non-covalently bound to the protein, they are possible to be separated from the protein by thermal denaturation. RP-HPLC chromatographies were monitored by following the UV-Vis absorbance spectrum of the eluted samples.

The chromatograms that are shown in the supplementary materials in figure 7.1 , show that G3PQO and PQO had FAD as a cofactor, while DHOQO presented FMN as cofactor. The order of polarity, and therefore the sequential order of elution, was FAD > FMN.

The retention time of the FAD, FMN and TPP is represented in table 4.1. Although, the protocol was not optimized for the identification of TPP (which causes the tailing effect observed in TPP elution), we aimed only to verify the presence or absence of the TPP. The absence of TPP was observed. This fact can mean this cofactor may have been lost during the purification process.

Table 4.1- Retention time of FAD, FMN, TPP and of the three proteins (DHOQO, G3PQO and PQO) injected in a Luna C18 column 3 µm (150 × 4.60 mm) operated in a HPLC system. The column was equilibrated with buffer A, 5 mM ammonium sulfate. The elution was performed using the buffer B, 5 % methanol. The sample was eluted in the same buffer with an isocratic gradient from 10 to 80 % of methanol at 1 mL $^{-1}$ min $^{-1}$. Solutions of 100 µM of FAD, FMN and TPP were used as standards.

	Retention time (min)
FAD	**12.0**
FMN	**12.5**
TPP	**3.75**
DHOQO	12.5
G3PQO	12.0
PQO	12.0

4.3.3. Oligomerization State identification

The oligomerization state of the proteins was investigated by performing a Native-PAGE Novex 4-16 % Bis-Tris Gel. This type of gel system is a neutral pH, polyacrylamide mini gel system, allowing to perform native (non-denaturating) electrophoresis. This technique provides a sensitive and high-resolution method for analysis of molecular mass estimations and assessing the purity of native proteins. In this type of electrophoresis Coomassie G-250 binds to proteins and confers a negative charge while maintaining the proteins in their native state without any protein denaturation.

The theoretical masses of the G3PQO and PQO are 62 kDa and 63 kDa, respectively. The DHOQO is described as a 39 kDa protein. The native gel indicates that the G3PQO and the PQO were present in the form of a dimer appearing a band at below the 140 kDa band of the marker. By contrast, the DHOQO appeared to be a monomer presenting a band below of the 66 kDa of marker band.

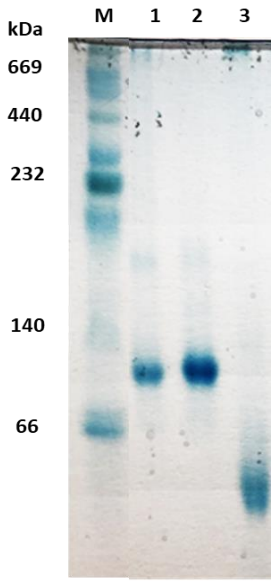

Figure 4.7- Native-PAGE Novex 4-16 % Bis-Tris Gel. Lane 1 - PQO; Lane 2 - G3PQO; Lane 3- DHOQO. The High Molecular Weight Calibration (HMW) kit was used as protein mass marker ranging from 66 to 669 kDa.

4.3.4. Protein reduction and reoxidation

The obtained UV-visible spectra for DHOQO, G3PQO and PQO were similar between them, and characteristic of a flavin spectrum. The spectra are presented in figure 7.2 in the supplementary materials.

The reduction of 6 µM of DHOQO was achieved by addition of the 6 µM of electron donor, dihydroorotate, in 50 mM K_2HPO_4/KH_2PO_4 pH 7.0, 250 mM NaCl buffer. The reoxidation of the protein was performed by addition of the electron acceptor, DMN in equal proportions. Since flavoproteins are characteristically reactive with molecular oxygen, anaerobic conditions have to be imposed during these assays. O_2-free conditions were obtained by using a scavenging system, composed by two enzymes (Glucose oxidase and Catalase) that consume glucose and turn molecular oxygen in water in two reactions, as shown in supplementary materials in figure 7.3. The same was tested to the other two proteins, G3PQO and PQO, in the same conditions, but no reduction and thus no reoxidation was observed. This situation can be explained by the fact of the conditions tested are not the optimal conditions for these experiments. An optimization process was needed, such as testing different pH values, different buffers or the presence of other cofactors, as Mg^{2+} and TPP to the PQO case [34] or the presence of the detergents or liposomes in the case of the G3PQO [35].

In the figure 4.8, are represented the UV-Visible spectra of both the oxidized and reduced forms of DHOQO. The obtained spectrum represented by the black filled line, corresponds to the oxidized DHOQO, and presented an expected flavin protein absorbance spectrum with maxima at 280 nm (from the aromatic amino acid residues), 375 nm and 450 nm (from the flavin cofactor).

In the case of DHOQO it was possible to achieve full reduction (represented by the grey dashed line) by addition of dihydroorotate with a 1:1 ratio (protein: substrate). The reduction was characterized spectroscopically by the decrease in the absorption at 375 nm and 450 nm.

The reoxidation of the protein was obtained by adding a menaquinone analogue, DMN, in equal amounts to dihydroorotate. Reoxidation is manifested by the return of the absorbance intensities to the previous values. This allowed to conclude that the purified DHOQO is redox active.

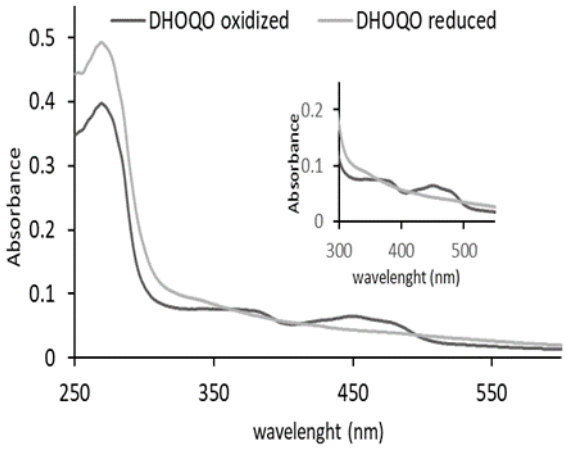

Figure 4.8-Absorption spectra of DHOQO from *S. aureus* oxidized (black line) and reduced with dihydroorotate (grey line). The reduction of 6 µM of DHOQO was achieved by addition of the 6 µM of electron donor, dihydroorotate, in 50 mM K_2HPO_4/KH_2PO_4 pH 7.0, 250 mM NaCl buffer. O_2-free conditions were obtained by using a scavenging system.

4.3.5. Enzymatic activity assays

As the G3PQO and PQO were not reduced by the respective substrates in the conditions tested and thus optimization of the assay conditions are needed, we decided advance with the kinetic characterization of only the DHOQO.

The enzymatic activity of the fraction 1 of the purified DHOQO was tested with excess of substrates. 150 µM of DMN was used as electron acceptor and 150 µM of dihydroorotate was used as electron donor. These activities were performed following the change in the absorbance of DMN at 270 nm, because it is the point at which the difference between the oxidized DMN and reduced DMN is the highest. The spectra of the oxidized and reduced DMN are represent in figure 7.4 in supplementary materials.

DHOQO showed dihydroorotate:quinone oxidoreductase activity, 8.53 ± 0.23 µmol min^{-1} mg^{-1} (Figure 4.9A), which was affect by the presence of HQNO, a quinone reductase inhibitor. In this case in the activity of the DHOQO decreased to 0.43 ± 0.20 µmol min^{-1} mg^{-1} (Figure 4.9B).

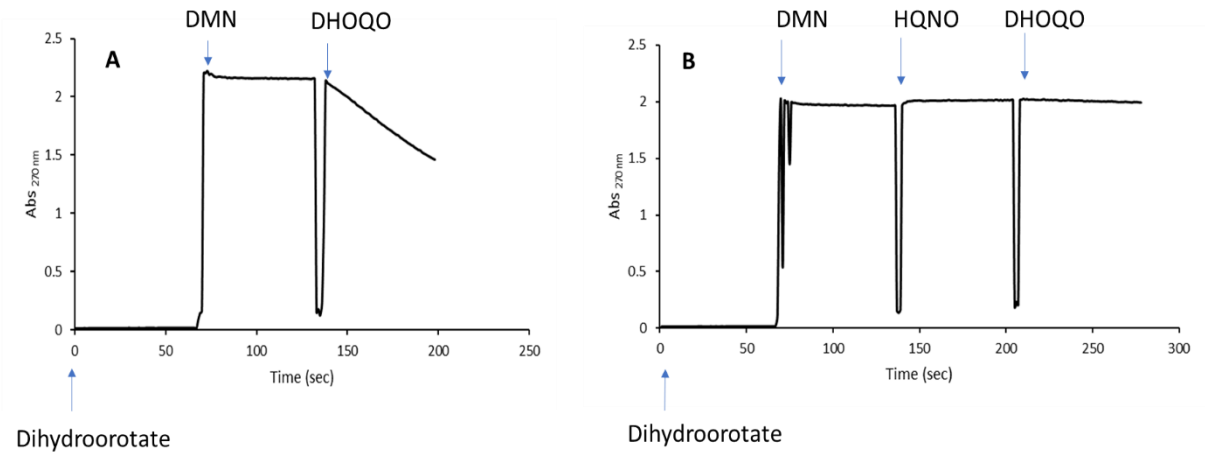

Figure 4.9- A- Dihydroorotate: quinone oxidoreductase activity, using 150 µM of dihydroorotate and DMN in 50 mM K_2HPO_4/KH_2PO_4 pH 7.0, 250 mM NaCl buffer. B- Dihydroorotate: quinone oxidoreductase activity in the presence of 100 µM HQNO. The specific activity was measured following the DMN at 270 nm.

4.3.6. pH profile

Enzymatic activities were tested at different pH values, with the goal of determining, which is the optimal pH for the enzymatic activity to occur. Assays were performed in duplicates at 37 ºC and following the change in absorbance of DMN at 270 nm. The range of pH tested was 5.5 to 9 in 50 mM MES, 50 mM Bis-Tris Propane, 250 mM NaCl buffer. The pH for which the protein presented the highest activity was 7.5 (Shown in figure 4.10).

Since the *Staphylococcus aureus* is a bacterium that growths at neutral pH and the pH of the cells is also around 7, the fact of the maxima activity of the DHOQO was observed at pH 7.5 is according these conditions.

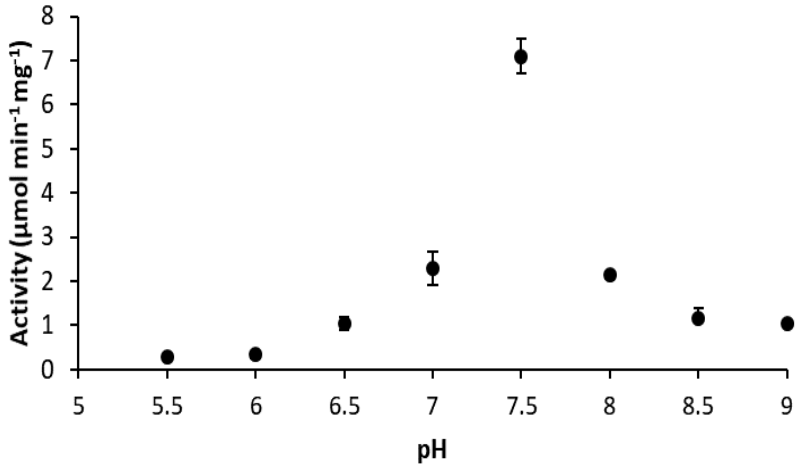

Figure 4.10- pH dependent enzyme activity of DHOQO from Staphylococcus aureus. Each point is representative of two experiments, using 150 µM of dihydroorotate, 150 µM of DMN and 0.125 µM of the protein. All assays were measure using a scavenging system that ensured O_2-free conditions, at 37 ºC and under agitation. pH values between 5.5 and 9 were tested in 50 mM MES, 50 mM Bis-Tris Propane, 250 mM NaCl buffer. The specific enzyme activity was calculated based on the Lambert-Beer law and according to a molar extiction coefficient of DMN at 270 nm equivalent to17545 M^{-1} cm^{-1}.

4.3.7. Steady state kinetic studies

The dihydroorotate:quinone oxidoreductase activity was measured for the purified DHOQO (fraction 1). The reaction was monitored spectroscopically at 270 nm by measuring quinone reduction to the quinol form (extinction coefficient of DMN at 270 nm equivalent to 17545 M^{-1} cm^{-1}). Three independents experiments for each concentration were performed for each substrate, dihydroorotate and DMN. In one case, the concentration of DMN was kept constant and the titration of dihydroorotate was performed in range of 0 to 300 µM. In the second case the concentration of dihydroorotate was kept constant and the titration of DMN was done in range of 0 to 125 µM.

The specific enzymatic activity (µmol min^{-1} mg^{-1}) was measured and plotted vs substrate concentration. The kinetic parameters were obtained by fitting the Michaelis-Menten equation to the experimental points.

This model is described by the equation, $v_0 = \frac{v_{max}[S]}{K_m+[S]}$, which relates the reaction rate to the concentration of the substrate, whereas Vo is the initial rate, [S] is the substrate concentration, V_{max} is the value of the maximum velocity and K_m represent the concentration of substrate necessary to reaches half of the Vmax.

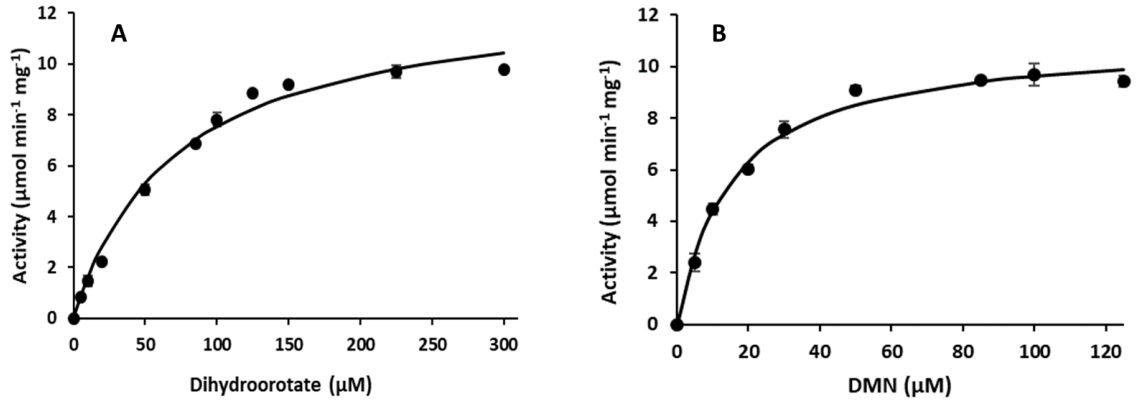

Figure 4.11- Steady-state analyses of the activity DHOQO from *S. aureus*. dihydroorotate:quinone oxidoreductase activity as function of the concentration of DMN (A) and dihydroorotate (B). The data points were fitted with a Michaelis-Menten equation (full line), $v_0 = \frac{v_{max}[S]}{K_m+[S]}$. The specific activity of the DHOQO was obtained following the DMN reduction at 270 nm.

The experimental points, as well as the calculated curves for the steady state kinetics are represented in the figure 4.11. The kinetics parameters were calculated using the solver program by fitting our data with the Michaelis- Menten equation (Shown in table 4.2).

In the case of the DMN titration, the measured V_o values seemed to tend to decrease in the highest concentrations (150 and 300 µM), what can suggest substrate inhibition. Other possible explanation to this observed fact might be the sensibility to the ethanol used to prepare the quinone solution.

Table 4.2- The kinetics parameters Km and Vmax of the DHOQO from the titrations of DMN and Dihydroorotate. The values were calculated fitting the data with the Michaelis-Menten equation.

DMN		Dihydroorotate	
K_m (µM)	**V_{max} (µmol min^{-1} mg^{-1})**	**K_m (µM)**	**V_{max} (µmol min^{-1} mg^{-1})**
15.5 ± 0.74	11.8 ± 0.03	71.6 ± 7.36	12.9 ± 0.46

The kinetics parameters indicate DHOQO needs the higher quantity of dihydroorotate than of the DMN to reaches the limit velocity of the reaction.

The inhibition of HQNO on the dihydroorotate:quinone oxidoreductase of the DHOQO was also tested. Two independent curves were performed. These assays were done by the addition of HQNO, in the range of 0 to 100 µM. The specific activity was obtained and was represented versus the HQNO concentration, in the curve shown below in the figure 4.12. From the titration curve it was possible to obtain the inhibition constant (K_i) using the equation $v_0^i = v_0^{max} \frac{\left(1+\beta\frac{[I]}{Ki}\right)}{\left(1+\frac{[I]}{Ki}\right)}$ to fitted the obtained data.

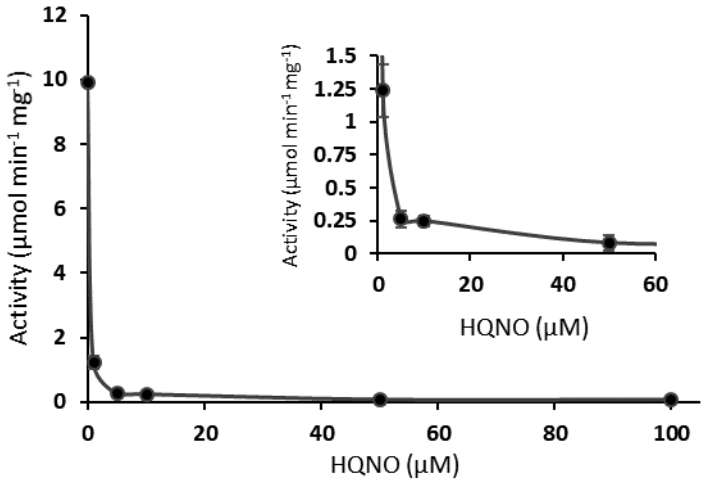

Figure 4.12- Steady-state analyses of the activity of DHOQO from S. aureus in the presence of HQNO. Dihydroorotate: quinone oxidoreductase activity as function of the concentration of the inhibitor HQNO, using as electron acceptor DMN. The data points were fitted using equation $v_0^i = v_0^{max} \frac{\left(1+\beta\frac{[I]}{Ki}\right)}{\left(1+\frac{[I]}{Ki}\right)}$ and the obtained was Ki = 0.13 µM ± 0.03 µM

The presence of information about these types of kinetic assays was not found in the literature to the DHOQO from *S. aureus.* This type of kinetic characterization were performed to DHOQO from parasites (*Plasmodium berghei*) [36], rat [37] and human [38]

4.3.8. Protein substrate interaction

In order to assess the substrate-enzyme interaction we performed fluorescence quenching studies using fluorescence spectroscopy to monitor changes in protein conformation caused by ligand interaction. These studies measured the decrease of the fluorescence emission intensities of the tryptophan residues as a function of substrate concentration.

Fluorescence quenching is a process that decreases the intensity of the fluorescence emission. Quenching may occur by several mechanisms. Most common ones are the dynamic or collisional quenching, where a random non-interactive collision of a small molecule deactivates the excited state of the fluorophore, and static quenching, where small molecule makes a ground state complex with the fluorophore so that it becomes nonfluorescent. The extent of dynamic quenching depends on the accessibility of the fluorophore to the quencher. The quenching agents in these studies were the substrates tested, since the binding to the proteins may induce conformational changes that may, potentially influencing tryptophan surrounding environment [39].

The excitation wavelength selected was 295 nm, to selectively excite the tryptophans, in order exclude a possible inner filter effect. This effect results from the absorption of the quinones at 280 nm. The emission spectra of each protein were recorded at around 350 nm, the spectra are represented in figure 7.5 in supplementary materials.

During the addition of each substrate a decrease in the intensity of fluorescence emission at 350 nm was observed. This decrease in emission (% ΔF_{max}) was normalized and plotted versus the substrate concentration.
From these assays the dissociation constant, K_D, was obtained, using the Monod-Wyman-Changeux (MWC) model equation [40], $\Delta F = \Delta F^{max} \times \frac{\frac{[S]}{K_S}\left(1+\frac{[S]}{K_S}\right)}{L+\left(1+\frac{[S]}{K_S}\right)^2}$, whereas ΔF is a difference of fluorescence emission; ΔF^{max} is a difference of the maximum fluorescence emission; [S] is the substrate concentration; Ks is the dissociation constant and L is the allosteric constant. This model considers proteins as an oligomer of protomers, with each protomer able to exist in either a tense or a relaxed state (which the relaxed state has the highest affinity to the ligand). The model allows to consider an allosteric effect regarding the binding of the ligand to the protein. If a dissociation constant is high, it means that the propensity of ligand to dissociate of the protein is also high, more specifically, it tends to be weakly bound to the protein, meaning a low affinity.

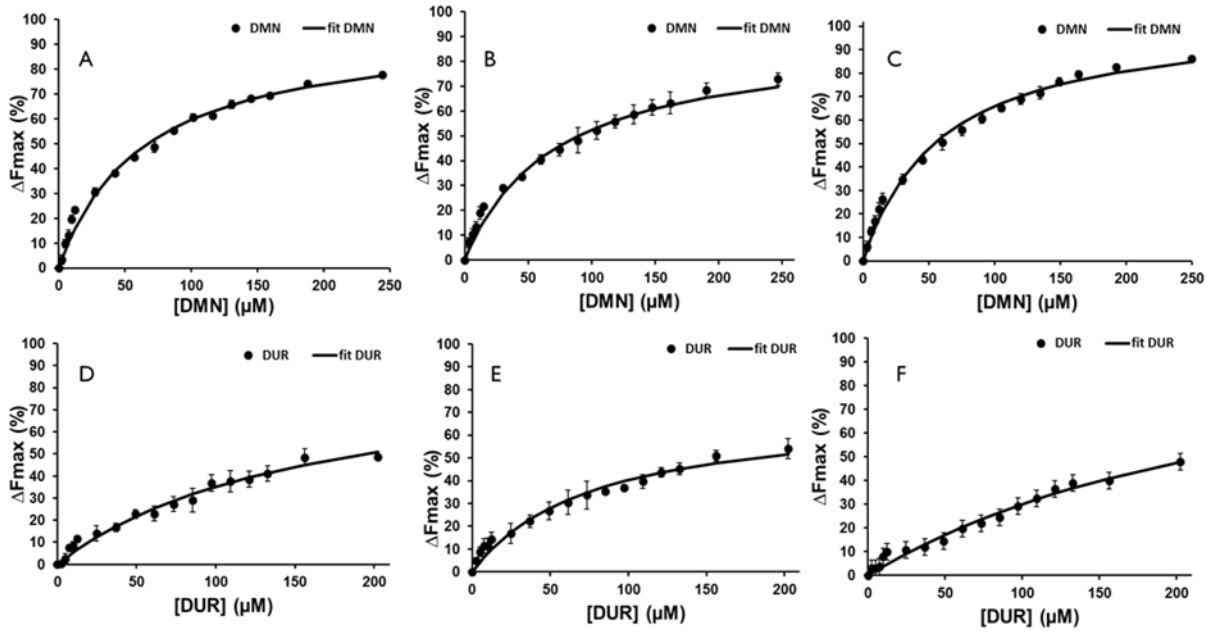

Figure 4.13- Protein-substrate interaction curves, representing the % fluorescence intensity quenching versus substrate concentration for DHOQO, G3PQO and PQO. The fluorescence quenching studies of the three proteins were performed with excitation wavelength at 295 nm. A, B and C- substrate interaction between DHOQO, G3PQO and PQO and DMN, respectively; D, E and F- substrate interaction between DHOQO, G3PQO and PQO and duroquinone, respectively. The solid lines were obtained by fitting the Monod-Wyman-Changeux (MWC) model equation, $\Delta F = \Delta F^{max} \times \frac{\frac{[S]}{K_S}\left(1+\frac{[S]}{K_S}\right)}{L+\left(1+\frac{[S]}{K_S}\right)^2}$

Conformational changes in the protein due to interactions with DMN (2,3- Dimethyl-1,4-naphthoquinone) and DUR (Duroquinone) were investigated. DMN is a naphthoquinone (a menaquinone analogue), characterized by a bicyclic ring system. DUR is a benzoquinone that presents only one ring.

The dissociation constants of DHOQO, G3PQO and PQO for DMN were lower than for DUR, indicating higher affinity of the proteins to DMN. A % ΔFmax around 80 % was obtained to the titration with DMN, whereas for the DUR the maximum was around 50 %, which could indicate a different type of interaction between the proteins and the two different quinones. The higher affinity observed for DMN is in agreement with the fact that *S. aureus* presents menaquinone as its physiological quinone. The results are shown in the table 4.3. below and the curves are presented in figure 4.13.

Table 4.3- The K_D values and % Δ Fmax of DHOQO, G3PQO and PQO from the titrations with DMN and Duroquinone from the fluorescence quenching studies.

	DMN		DUR	
	K_D	% Δ F_{max}	K_D	% Δ F_{max}
DHOQO	63.6 ± 7.6	77.8 ± 3.9	157.8 ± 5.87	48.6 ± 14.1
G3PQO	63.1 ± 5.9	72.9 ± 3.7	133.8 ± 22.2	54.1 ± 1.4
PQO	59.1 ± 5.2	86.2 ± 0.3	190.2 ± 16.6	47.8 ± 17.0

Observing the interaction between the proteins and the respective electron donor represented in figure 4.14, we conclude that the affinity between PQO and pyruvate, and DHOQO and dihydroorotate seem to be similar, presenting in both cases a close K_D value. The G3PQO presents a higher affinity for the electron donor, presenting the lower K_D in comparison to other proteins.

The K_D of 53.7 ± 3.00 µM (Shown in table 4.4) was obtained to the interaction between the PQO and pyruvate. The K_D to interaction PQO- pyruvate was also determined by *Zhang et al*. The value of K_D obtained in their experiments was 26.2 µM, which is a lower value compared with the obtained in our experiments. In our assays we tested the interaction the protein only with pyruvate , but *Zhang et al*, tested the same interaction but in the presence of TPP and Mg^{2+} in solution [41] . The higher affinity of the pyruvate to the PQO demonstrated in their assays, can be explained by the presence of the Mg^{2+} and TPP, other cofactors of the PQO, that could induce a different conformation that facilitate the interaction of the pyruvate with the protein [34].

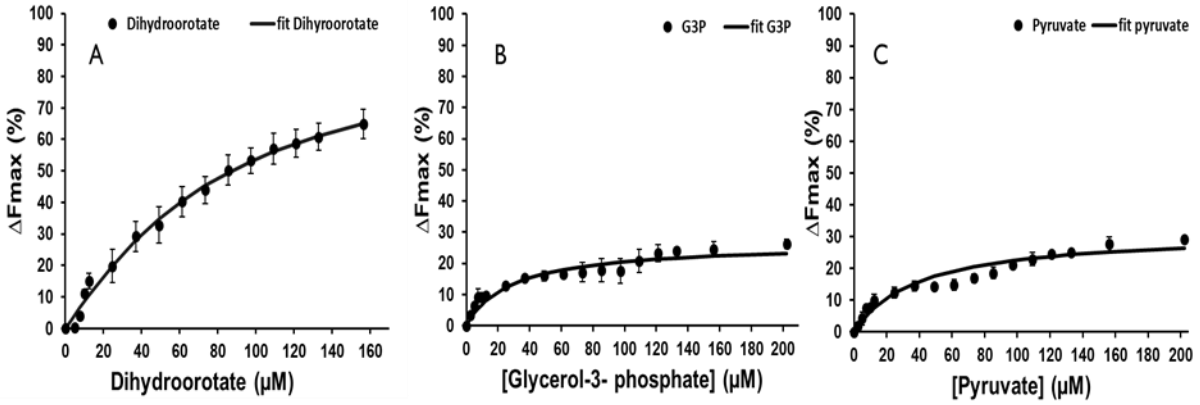

Figure 4.14- Protein- substrate interaction curves, representing the % fluorescence intensity quenching versus substrate concentration for DHOQO, G3PQO and PQO. The fluorescence quenching studies of the three proteins were performed with excitation wavelength at 295 nm. A- substrate interaction between DHOQO and dihydroorotate; B- substrate interaction between G3PQO and glycrol-3 – phosphate; C- substrate interaction between PQO and pyruvate ; The solid lines were obtained by fitting the Monod-Wyman-Changeux (MWC) model equation, $\Delta F = \Delta F^{max} \times \frac{\frac{[S]}{K_S}\left(1+\frac{[S]}{K_S}\right)}{L+\left(1+\frac{[S]}{K_S}\right)^2}$.

Table 4.4- The K_D values and ΔF_{max} of the DHOQO, G3PQO and PQO from the titrations with each electron donor, from the fluorescence quenching studies.

DHOQO-Dihy		**G3PQO- G3P**		**PQO-Pyruvate**	
K_D	% Δ Fmax	K_D	% Δ Fmax	K_D	% Δ Fmax
60.8 ± 4.1	64.9 ± 5.46	23.8 ± 2.7	26.3 ± 2.5	53.7 ± 3.00	29.1 ± 2.87

The titration with HQNO allowed determining its K_D. This information is important for the titrations where HQNO is present simultaneously with other ligands. The obtained K_D indicates a higher affinity of the protein to HQNO. These data agree with the higher inhibition of HQNO observed in the enzymatic kinetics and in the steady state kinetics.

In the case of DHOQO, to complement the results obtained in the enzyme kinetics studies, the titrations of DMN and dihydroorotate in presence of HQNO were performed. The titrations of DMN and dihydroorotate, in the case of DHOQO, with the presence of HQNO were performed, in order to understand if the HQNO influences the interaction of each substrate with the protein. The curves represented in figure 4.15 show the titrations of the DMN and Dihydroorotate in the presence of HQNO. Observing the K_D values in table 4.5 it is visible that HQNO influences the binding of DMN, since there is a change on the K_D value and in the % Δ Fmax (figure 4.15B). This indicates that the HQNO influences the environment of the tryptophans in the vicinity of the DMN pocket. In the case of the Dihydroorotate, the inhibitor seems not to influence the interaction, since the curves superimpose and the K_D value remained practically the same (figure 4.15C).

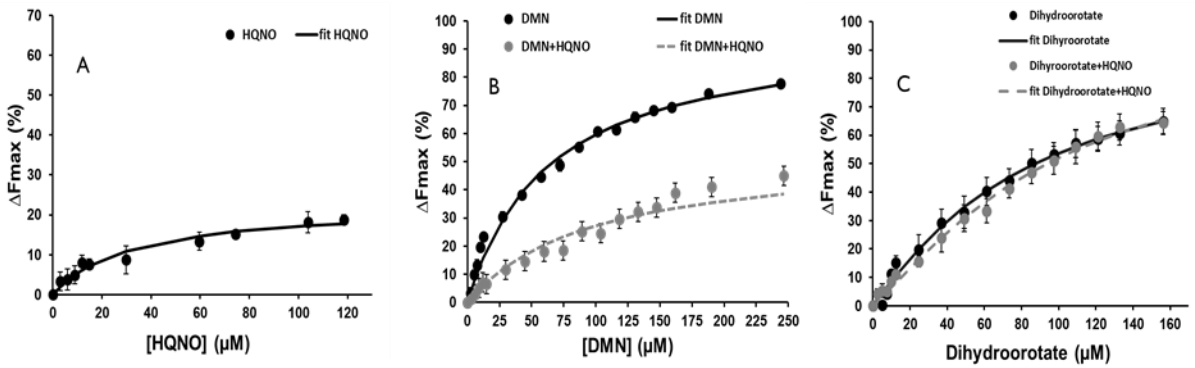

Figure 4.15 - Protein- substrate interaction curves, representing the % fluorescence intensity quenching versus substrate concentration for DHOQO. The fluorescence quenching studies of the DHOQO were performed with excitation wavelength at 295 nm. A- substrate interaction between DHOQO and HQNO; B- substrate interaction between DHOQO and DMN in absence (black line) and in the presence of HQNO (grey line) ; C- substrate interaction between DHOQO and dihydroorotate in absence (black line) and presence of HQNO (grey line) ; The solid lines were obtained by fitting the Monod-Wyman-Changeux (MWC) model equation, $\Delta F = \Delta F^{max} \times \frac{\frac{[S]}{K_S}\left(1+\frac{[S]}{K_S}\right)}{L+\left(1+\frac{[S]}{K_S}\right)^2}$

This result could mean that the DMN and dihydroorotate binds at different binding sites and that HQNO could have an effect in the binding site of the DMN, and not of the dihydroorotate. Another explanation would be HQNO and the quinone sharing the same binding pocket, which has been showed in other quinone reductases [42].

Table 4.5- The K_D values and % ΔF_{max} of DHOQO from the titrations with HQNO and DMN and Dihydroorotate in the presence of HQNO, from the fluorescence quenching studies.

	HQNO		**DMN+ HQNO**		**Dihy+HQNO**	
	K_D	**% ΔF_{max}**	**K_D**	**% ΔF_{max}**	**K_D**	**% ΔF_{max}**
DHOQO	32.4 ± 13.0	18.8 ± 4.5	96.21 ± 12.5	45 ± 4.7	57.8 ± 6.2	64.9 ± 4.0

The flavin fluorescence (emission at 530 nm) was also performed and did not change significantly in the presence of each substrate indicating that substrate binding does not induce protein conformational changes in the immediate vicinity of flavin cofactor. The emission at 530 nm was also recorded to control if the quenching observed is a consequence of the interaction between the protein and the substrates or a consequence of the dilution.

4.4. Cellular characterization

4.4.1. Construction of knockouts mutants DHOQO, G3PQO and PQO

The objective of the metabolic characterization was to study the cellular function of the three target quinone reductases (DHOQO, G3PQO and PQO). The approach used to achieve this was the construction of the respective knockouts mutants. The genes encoding for the three proteins were deleted by homologous recombination that occurs during the transduction process.

In general, strains of *S. aureus* have an impenetrable restriction barrier preventing the uptake of foreign DNA, and because of that, one of the limitations in the genetic manipulation of *S. aureus* is the fact that there is only a single strain available which can easily accept plasmid DNA isolated from *E. coli*. This strain, RN4220, is a chemical mutant obtained by high mutagenizing of the strain RN450 with nitrosoguanidine, and selection for a mutant that was able to accept and maintain *S. aureus* plasmids. For this reason, RN4220 has become an essential intermediate for laboratory manipulation of *S. aureus*. DNA plasmids first introduced into RN4220 by electroporation can be then transferred to other stains using the transduction process [43] [44] .

The process of the construction of the knockouts mutants involved 5 main steps: 1) amplification of the up and down fragments of the respected gene by PCR; 2) join these fragments using overlapping PCR; 3) cloning the product of the overlapping PCR into pMAD vector; 4) electroporation into *S.aureus* RN4220; 5) transduction (using the phage 88α) *S. aureus* MW2 [45].

1st Step - Amplification of the up and down fragments

The up and the down fragments were amplified at 1300 bp upstream and downstream of the gene encoding for each protein. These two different fragments were amplified by PCR, using the Phusion Polymerase, the genomic DNA of the strain USA300 as template, and the pair of primers P1/P2 and P3/P4.

In table 7.1 in the supplementary materials, was represented the melting temperature, the primers and annealing temperature for the three proteins.

PCR product formation was evaluated by agarose gel electrophoresis. Observing the 1 % agarose gel in the figure 4.17, it is visible the presence of the one band at approximately 1300 bp for the DHOQO, G3PQO and PQO, which means the amplifications of the up and down fragments were successfully obtained for the three protein under study. These PCR products were purified using the Wizard SV gel and PCR clean-up system (Promega).

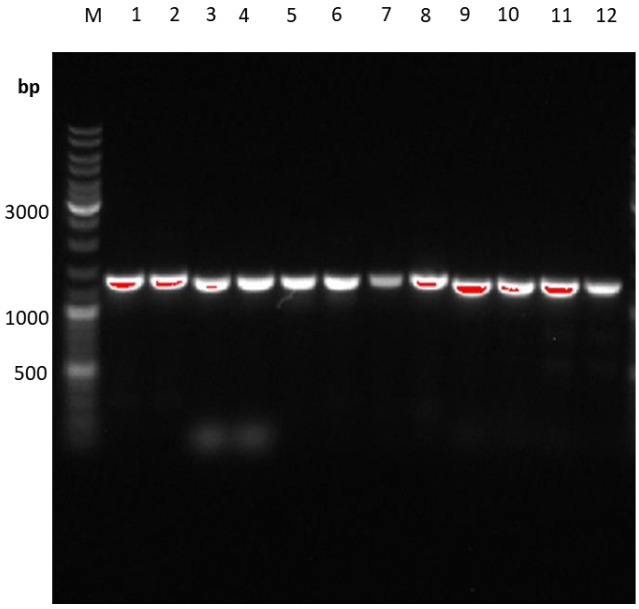

Figure 4.17 - 1 % agarose gel of the amplification of up and down fragments for the DHOQO KO, G3PQO KO and PQO KO. Lanes 1 and 2 are G3PQO up fragment; Lanes 3 and 4 are G3PQO down fragment; Lanes 5 and 6 are PQO up fragment; Lanes 7 and 8 are PQO down fragment; Lanes 9 and 10 are DHQO up fragment; Lanes 11 and 12 are DHOQO down fragment. The GeneRuler DNA Ladder mix was used as marker.

The analysis of the purity of these PCR products was performed using a NanoDrop spectrophotometer and the ratios between 260/280 nm and 260/ 230 nm were calculated.

The ratio of absorbances at 260 and 280 nm is used to assess the purity of DNA and RNA. A ratio of approximately 1.8 is generally accepted as pure for the DNA containing samples. If the ratio is lower it may indicate the presence of proteins, phenol or other contaminants that absorb strongly at or near 280 nm. The ratio between 260/230 nm is used as a secondary measure of nucleic acid purity. Values in the range of 2.0-2.2. are commonly acceptable as indicative of a pure sample. A lower ratio can indicate the presence of EDTA, carbohydrates or phenol.

Table 4.6 - The ratios between absorbance at 260 nm and 280 nm (A260/A280) and between 260 and 230 nm (A260/A230) for the purified PCR products of DHOQO, G3PQO and PQO.

	up fragment			**down fragment**		
	[DNA] ng/µL	**A260/A280**	**A260/A230**	**[DNA] ng/µL**	**A260/A280**	**A260/A230**
DHOQO	63.80	1.87	2.72	69.70	1.87	2.72
G3PQO	71.50	1.90	2.08	73.50	1.87	2.06
PQO	40.00	1.85	1.75	77.30	1.91	2.59

The obtained ratios for the purified up and down fragments of DHOQO, G3PQO and PQO are shown in table 4.6. We concluded that the obtained ratios were around the acceptable values and it was possible to consider that the analyzed samples were pure, allowing us to advance for the next steps.

2nd Step - Overlapping PCR of the up and down fragments

For this step a lot of trials optimization had to be performed to achieve optimization for obtaining a significant amount of purified DNA needed to advance to the next steps. The first tested variables in the PCR conditions were: extension time, annealing temperature (increasing/decreasing the theoretical annealing temperature), primer concentration and reaction mixture volume.

In this step, the obtained up and down fragments for each protein were joined using the Overlapping PCR. These PCRs used an initial denaturation at 98 ºC, followed by 30 cycles of an annealing step at 62-66ºC for 30 seconds, an elongation step at 72 ºC for 1 minute and 25 seconds.

In the gel shown in figure 4.18 was visible a band in around of 2500 bp region is visible, which is an expected size of the resulted fragment, indicate the successfully amplification of the overlap fragment for DHOQO, G3PQO and PQO in two different annealing temperature tested.

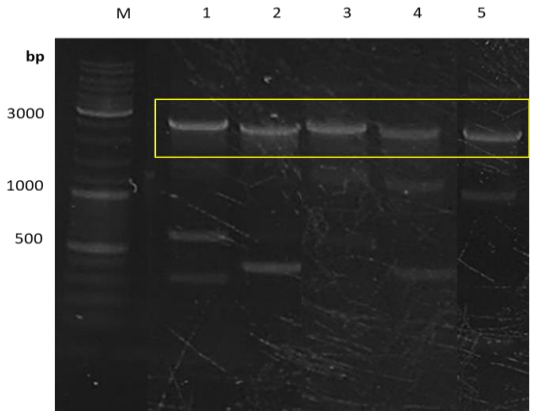

Figure 4.18 -1% agarose gel of the amplification of the overlap fragments for the DHOQO KO, G3PQO KO and PQO KO. Lane 1 - DHOQO (66 ºC); Lane 2 - PQO (66ºC); Lane 3 - DHOQO (62 ºC); Lane 4 - PQO (62ºC); Lane 5 - G3PQO (62ºC); The GeneRuler DNA Ladder mix was used as marker.

3rd Step - Cloning the insert into pMAD vector

The next step involved the cloning of the up-down fragment into pMAD vector. This vector was developed to facilitate isolation of allelic replacement mutants in Gram-positive bacteria including *S. aureus.* pMAD carries the pE194ts ori and *bgaB* gene, encoding thermostable β-galactosidase. The bgaB expression allows staphylococci to cleave the chromogenic substrate X-gal, thereby generating colonies with blue color. Although this technique does not affect neither frequency nor selection of mutations, it provides a screening tool for excision and loss of plasmid [46].

The cloned plasmids were isolated from *E. coli* DC10B. The plasmids extracted can be directly transformed into *S. aureus*, since not they have a cytosine methylation which facilitate the bypass of the type IV barrier [47].

Regarding the cloning process, we first digested the insert (fragment up-down) and the pMAD with restriction enzymes. Then, we ligated the insert and the vector using the T4 DNA ligase (Promega). The digestion process was done for 2 hours and 30 minutes at 37 ºC.

The ligation of the digested pMAD plasmid and insert was done with a proportion of 6:3 (insert: plasmid) using a T4 Ligase (Promega) and incubated using two different approaches: for 3 hours at room temperature; and for 16 hours at 4 ºC. The agarose gel shown below presents a band at 9600 bp that corresponds to the pMAD digested with XmaI and MluI and with XmaI and SlaI, for DHOQO and G3PQO, respectively. The band corresponding to the insert (fragment up-down) of DHOQO and digested pMAD are presented in the figure 4.19.

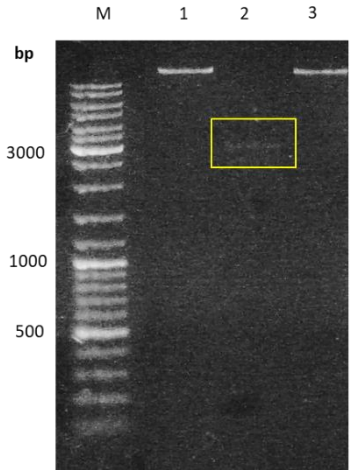

Figure 4.19 - 1% agarose gel showing the digestion of the pMAD and inserts of the DHOQO KO and G3PQO KO. Lane 1 - pMAD digested with XmaI and SalI; Lane 2- insert of DHOQO; Lane 3 - pMAD digested with XmaI and MluI; The GeneRuler DNA Ladder mix was used as marker.

After the incubation was completed, 5 µL of the final mixture was transformed into *E. coli* DC10B using the heat shock protocol.

The reaction mixture without the insert was prepared in order to perform the auto ligation control. It was important that the number of colonies in the control plates was less than in the ligation plates, since the auto ligation process should not have occurred.

In case of the DHOQO KO and G3PQO KO the number of colonies in the ligation plates was higher than in the control plates, but in the case of the PQO KO this was not verified. A possible explanation to the fact of all colonies tested from the ligation plates were all negative, is the concentration of DNA (insert) purified was low or the presence of contaminants (ethanol or phenol) caused the inhibition of the T4 DNA ligase. Figure 4.20 displays the agarose gels showing the presence of the bands in the region of the 2500 bp, which represent the presence of the insert, confirming the positive colonies for the DHOQO and G3PQO.

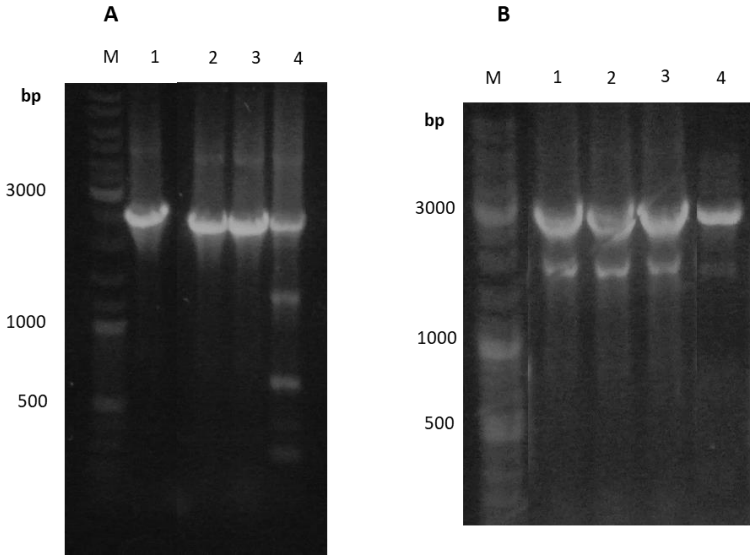

Figure 4.20 - 1% agarose gel of the screening of the transformed colonies by PCR. Confirmation the presence of the construct pMAD+ insert for the case of the DHOQO (A) and G3PQO (B). The primers pMAD forward and pMAD reverse were used. The bands correspond of the amplification of the fragment of interest (2500 bp), and confirming the successfully transformation and cloning the pMAD construct into *E. coli* DC10B. The GeneRuler DNA Ladder mix was used as marker.

The cloned plasmid was extracted from the positive colonies using the ZR Plasmid Minipreps-classic (ZYMO RESEARCH). The purity of the obtained plasmids was analyzed using a NanoDrop spectrophotometer. The positive colony for the presence of the construct of DHOQO and G3PQO that presented, the best ratios (A260/A280; A260/A230) and concentration of DNA was chosen to be sequenced. The results are shown in table 7.2 in supplementary materials.

For DHOQO KO, in order to confirm the presence of the construct (pMAD + insert), the extracted plasmids were digested by XmaI and MluI and loaded in the agarose gel. The figure 4.21 shows two bands: one around 9600 bp corresponding to the pMAD vector; and a second one corresponding to the insert in the region of 2555 bp. This served as another confirmation that the insert was cloned into the pMAD.

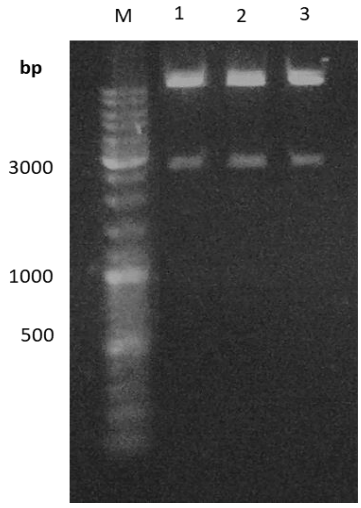

Figure 4.21 -1% agarose gel of the digestion of the construct of pMAD + insert of DHOQO KO. Lane 1,2 and 3 – pMAD band at 9600 bp and insert band at 2555 bp region. The primers p1-DHOQO and p4-DHOQO were used. The presence of the two bands in the expected regions, confirming the successfully construction and extraction of the pMAD+ insert $_{DHOQO}$. The GeneRuler DNA Ladder mix was used as marker.

4th /5th Steps – Electroporation (*S. aureus* RN4220) and Transduction *(S. aureus MW2*)

The fourth step was the electroporation of the obtained plasmid into *S. aureus* RN4220. To this step only advanced the DHOQO and G3PQO, since was not obtained the cloning of the fragment up- down into pMAD for the PQO protein.

In this step, 50 µL of competent cells of *S. aureus* RN4220 were mixed with 5 µL of the replicative plasmid pMAD extracted from E. coli DC10B in a 2.0 mm electroporation cuvette (Bio-Rad) and subjected to an electroporation pulse in a Gene Pulser Xcell equipment (Bio-Rad) set to 2.5 kV, 25 µF and 100 Ω [48] .The selection was done by inoculating the electroporated cells in TSA plates with erythromycin and X-gal, kept at 30 ºC. The resulting plates had blue colored colonies obtained because of the metabolization of the X-gal substrate.

After selection the transduction of the plasmid (into the *S. aureus* MW2 strain using the phage 88α) was performed. Transduction is the process by which any bacterial gene may be transferred to another bacterium via a bacteriophage by infection of the recipient bacterial host and recombination onto the chromosome followed by the phenotypic expression of the transferred DNA.

The recombination and integration of the plasmids into the chromosome was achieved by a two-step homologous recombination process. In the first step, recombinants were selected at the non-permissive temperature (for plasmid replication of 43 °C), using erythromycin and light blue colony color. In the second step, cells were incubated at the permissive temperature of 30 °C in the absence of antibiotic selection. From this step, resulted white and erythromycin-sensitive colonies in which the vector had been excised [49] .

Figure 4.22 shows an 1% agarose gel where is possible to observe a band around 2598 bp that confirmed the obtention of the knockout mutant of DHOQO (ΔDHOQO). The obtention of the mutant was confirmed by PCR and sequencing.

In the case of the G3PQO, the excision was not successful, since all tested colonies were excised to wild-type form, this could indicate that this protein are essential to the organism.

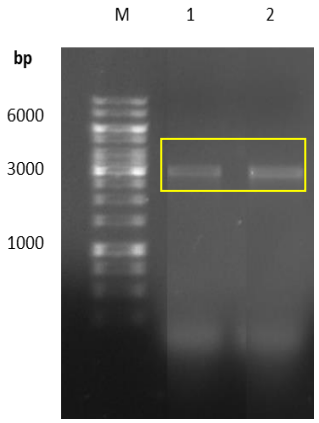

Figure 4.22 - 1% agarose gel of screening by PCR of the recombinants obtained to confirmation of the obtention of the knockout mutant ΔDHOQO strain. The primers p1-DHOQO and p4-DHOQO were used. The presence of the one band (2598 bp) in lane 1 and 2confirming the amplification of the fragment of interest and confirming the successfully excision of the pMAD into *S. aureus* MW2. The GeneRuler DNA Ladder mix was used as marker.

4.4.2. Cell growth studies

S. aureus growths were performed for the wild-type MW2 strain and for the obtained knockout mutant of the DHOQO protein (ΔDHOQO) in order to study the relevance and the impact of this protein in the energetic metabolism of *S. aureus.* Growths were followed by monitoring: $OD_{600\ nm}$ and the medium pH values.

In the WT growth the maximum $OD_{600\ nm}$ reached was ~ 7 after 7.5 hours of growth (figure 4.23, panel A, yellow points). The pH profile shows a continuous decrease since the beginning of the growth until approximately 6 hours of growth, followed by a slower pH rise growth (figure 4.23, panel B, yellow points). The minimum pH value observed was 5.38 (at 6 h of growth), having recovered from this initial pH drop by the end of the overnight growth.

Figure 4.23 shows that the growth of the knockout mutant (ΔDHOQO) reached a maximum $OD_{600\ nm}$ of 3 at 4.5 hours growth (figure 4.23, panel A, yellow points). Similarly to the observed for WT, the pH value decreased since the beginning of the growth until approximately 7.5 hours of the growth, but it did do recover staying constant at 5.4 (figure 4.23, panel A, blue points).

The results presented show a difference between WT and ΔDHOQO which reached stationary phase much earlier, revealing a different phenotype. Another difference was the pH profile of the two strain in study during growth. In the case of ΔDHOQO, pH decrease in the slowly rate until of 11 hours of the growth.

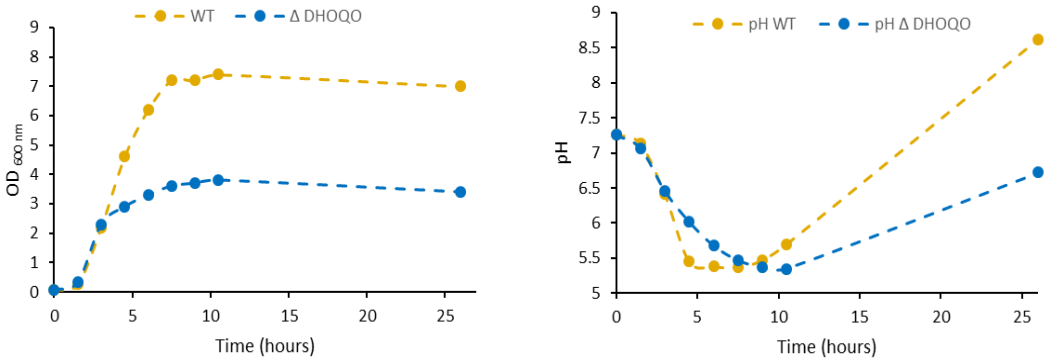

Figure 4.23- Growth of WT strain (yellow color) and ΔDHOQO (blue color) of *S. aureus* MW2 in TSB medium (initial OD 0.05, in aerobic conditions). The optical density at 600 nm and pH values were measured at 1.5 hours intervals. The results presented are representative of three independent experiments.

5. Conclusion

Staphylococcus aureus strains are potentially lethal bacterial pathogens that have been considered a serious worldwide problem to public health, especially due to its multiple drug resistance, which makes it a versatile pathogen capable of causing a wide range of human diseases. For this reason, it is important to explore and understand not only the mechanism behind this resistance, but also the conditions that allow *S. aureus* to live and survive in different environments. We aimed to contribute to expand these borders knowledge, investigating three quinone reductases involved in the metabolism of *S. aureus*, specifically Dihydroorotate:quinone oxidoreductase (DHOQO), Glycerol-3-phosphate:quinone oxidoreductase (G3PQO) and Pyruvate:quinone oxidoreductase (PQO).

Protein biochemical characterization was performed for DHOQO, G3PQO and PQO. The study of DHOQO was complemented by a cellular approach involving the study of the behavior of knockout mutants. The three respiratory enzymes were spectroscopically characterized, tested for their stability, and investigated in respect to their oligomerization state. The respective prosthetic groups were also identified. DHOQO was also functionally characterized by steady state kinetics, pH profile and protein substrate interaction.

At the beginning of the work conducing to this dissertation, the proteins G3PQO and PQO were already purified. On the other hand, the DHOQO expression and purification needed to be optimized and performed. Expression tests were conducted and the optima conditions for the expression of the DHOQO from *Staphylococcus aureus* identified, which allowed the expression of sufficient amounts of protein followed by its successful purification.

All proteins under study presented a flavoprotein characteristics spectrum, but only the DHOQO was shown to be redox active, being possible to obtain the full reduction with the addition of a similar concentration of the dihydroorotate. The reoxidation was also achieved by addition of the DMN, electron acceptor. Enzymatic studies showed that DHOQO has maxima dihydroorotate: quinone oxidoreductase activity at pH 7.5 and its activity decrease in the presence of HQNO, verifying this enzyme is inhibited by the HQNO.

With the work presented here, we could demonstrate that DHOQO from *S. aureus* purified for the first time, is a monomeric and FMN containing enzyme. Study of protein substrate interaction, taking advantage from the fluorescence of the tryptophans residues, indicated that the binding of the two substrates, dihydroorotate and DMN, could take place at different sites, since the presence of the inhibitor HQNO seems affected only the interaction of the DMN with the enzyme. A cell growth using the knockout mutant of the DHOQO and a wild type strains of *S. aureus* MW2 were performed and revealed a different phenotype, since the mutant strain reached the stationary phase much earlier than WT strain. Our data showed that DHOQO seems to have a relevant role in the energetic metabolism of *S. aureus*.

In the case of G3PQO and PQO full reduction of the enzymes was not achieved, being optimization necessary, however, it was possible observed that these enzymes are dimeric proteins and presented a FAD as cofactor. The protein substrate interaction studies revealed a higher affinity of those enzymes and of DHOQO for DMN (menaquinone) than for the duroquinone (Benzoquinone). Our experiments are according to the fact of *S. aureus* synthetizing menaquinone naturally.

The work developed here on the study of the DHOQO, G3PQO and PQO from *S. aureus* opens new perspectives for future studies with these proteins. The optimization of the construction of the knockouts

of G3PQO and PQO is still needed. Exploring not only the role of these proteins but also the spatial localization and regulation of these protein in the membrane, using the promoter Phusion and mNeonGreen molecular biology approaches, adding to metabolic studies by ^{1}H-NMR of metabolites in different steps in the bacteria growth should be an interesting future work to increase the knowledge of the mechanism behind the metabolism of *S. aureus*. In addition, solving the protein structure of the three quinone reductases is also an important acquisition to elucidate at a molecular level the interaction between the protein and its substrates, being possible in this away to provide some answers on the role of these proteins and understand deeper the energetic metabolism of the *S. aureus*.

6. References

[1] Marreiros, B.C., Calisto, F., Castro, P.J., Duarte, A.M., Sena, F.V., Silva, A.F., Sousa, F.M., Teixeira, M., Refojo, P.N., and Pereira, M.M. (2016). Exploring membrane respiratory chains. *Biochimica et Biophysica Acta - Bioenergetics 1857*, 1039–1067

[2] Berg, J., Tymoczko, J., and Stryer, L. (2002). Biochemistry, 5th edition.

[3] Shimizu, K. (2013) Main metabolism, *Bacterial Cellular Metabolic Systems*, 1–54.

[4] Madeira, V.M.C. (2018). Overview of mitochondrial bioenergetics. *In Methods in Molecular Biology, (Humana Press Inc.)*, 1–6.

[5] Mitchell, P. (1961). Coupling of phosphorylation to electron and hydrogen transfer by a chemi-osmotic type of mechanism. *Nature* 191, 144–148.

[6] Berrisford, J.M., Baradaran, R., and Sazanov, L.A. (2016). Structure of bacterial respiratory complex i. *Biochimica et Biophysica Acta - Bioenergetics 1857*, 892–901.

[7] Cecchini, G. (2003). Function and Structure of Complex II of the Respiratory Chain. *Annual Review of Biochemistry* 72, 77–109.

[8] Iwata, S., Lee, J.W., Okada, K., Lee, J.K., Iwata, M., Rasmussen, B., Link, T.A., Ramaswamy, S., and Jap, B.K. (1998). Complete structure of the 11-subunit bovine mitochondrial cytochrome bc1 complex. *Science* 281, 64–71.

[9] Wirth, C., Brandt, U., Hunte, C., and Zickermann, V. (2016). Structure and function of mitochondrial complex i. *Biochimica et Biophysica Acta - Bioenergetics* 1857, 902–914

[10] Tong, S.Y.C., Davis, J.S., Eichenberger, E., Holland, T.L., and Fowler, V.G. (2015). Staphylococcus aureus infections: Epidemiology, pathophysiology, clinical manifestations, and management. *Clinical Microbiology Reviews* 28, 603–661.

[11] Hodille, E., Rose, W., Diep, B.A., Goutelle, S., Lina, G., and Dumitrescu, O. (2017). The role of antibiotics in modulating virulence in staphylococcus aureus. *Clinical Microbiology Reviews* 30, 887–917.

[12] Melter, O., and Radojevič, B. (2010). Small Colony Variants of *Staphylococcus aureus* - review. *Folia Microbiologica 55*, 548–558.

[13] Mayer, S., Steffen, W., Steuber, J., and Götz, F. (2015). The *staphylococcus aureus* nuoL-like protein MpsA contributes to the generation of membrane potential. *Journal of Bacteriology 197*, 794–806.

[14] Marcia, M., Langer, J.D., Parcej, D., Vogel, V., Peng, G., and Michel, H. (2010). Characterizing a monotopic membrane enzyme. Biochemical, enzymatic and crystallization studies on *Aquifex aeolicus* sulfide:quinone oxidoreductase. *Biochimica et Biophysica Acta - Biomembranes* 1798, 2114–2123.

[15] Norager, S., Jensen, K.F., Björnberg, O., and Larsen, S. (2002). *E. coli* dihydroorotate dehydrogenase reveals structural and functional distinctions between different classes of dihydroorotate dehydrogenases. *Structure* 10, 1211–1223.

[16] Larsen.J.N., and Jensen, K.F. (1985). Nucleotide sequence of the *pyr D* gene of *Escherichia coli* and characterization of the flavoprotein dihydroorotate dehydrogenase. *European Journal of Biochemistry* 151, 59–65.

[17] Liu, S., Neidhardt, E.A., Grossman, T.H., Ocain, T., and Clardy, J. (2000). Structures of human dihydroorotate dehydrogenase in complex with antiproliferative agents. *Structure* 8, 25–33.

[18] Wegener, M., Vogtmann, K., Huber, M., Laass, S., and Soppa, J. (2016). The *glpD* gene is a novel reporter gene for *E. coli* that is superior to established reporter genes like *lacZ* and *gusA*. *Journal of Microbiological Methods* 131, 181–187.

[19] Iuchi, S., Cole, S.T., and Lin, E.C.C. (1990). Multiple regulatory elements for the *glpA* operon encoding anaerobic glycerol-3-phosphate dehydrogenase and the *glpD* operon encoding aerobic glycerol-3-phosphate dehydrogenase in *Escherichia coli*: Further characterization of respiratory control. *Journal of Bacteriology* 172, 179–184.

[20] Schryvers, A., and Weiner, J.H. (1981). The anaerobic sn-glycerol-3-phosphate dehydrogenase of *Escherichia coli.* Purification and characterization. *Journal of Biological Chemistry* 256, 9959–9965.

[21] Rawls, K.S., Martin, J.H., and Maupin-Furlow, J.A. (2011). Activity and transcriptional regulation of bacterial protein-like glycerol-3-phosphate dehydrogenase of the haloarchaea in *Haloferax volcanii*. *Journal of Bacteriology* 193, 4469–4476.

[22] Mráček, T., Drahota, Z., and Houštěk, J. (2013). The function and the role of the mitochondrial glycerol-3-phosphate dehydrogenase in mammalian tissues. *Biochimica et Biophysica Acta - Bioenergetics* 1827, 401–410.

[23] Spoering, A.L., Vulić, M., and Lewis, K. (2006). GlpD and PlsB participate in persister cell formation in *Escherichia coli. Journal of Bacteriology* 188, 5136–5144.

[24] Zhang, X., Bayles, K.W., and Luca, S. (2017). *Staphylococcus aureus* CidC Is a Pyruvate:Menaquinone Oxidoreductase. *Biochemistry* 56, 4819–4829.

[25] Schreiner, M.E., and Eikmanns, B.J. (2005). Pyruvate:quinone oxidoreductase from *Corynebacterium glutamicum*: Purification and biochemical characterization. *Journal of Bacteriology* 187, 862–871.

[26] Mather, M.W., and Gennis, R.B. (1985). Spectroscopic studies of pyruvate oxidase flavoprotein from *Escherichia coli* trapped in the lipid-activated form by cross-linking. Journal of Biological Chemistry *260*, 10395–10397.

[27] Froger, A., and Hall, J.E. (2007). Transformation of Plasmid DNA into *E. coli* using the heat shock method. Journal of Visualized Experiments.

[28] Thermo Scientific (2011). User Guide: Pierce BCA Protein Assay Kit (MAN0011430 Rev. A). Pierce Biotechnology *0747*, 1–7.

[29] Aliverti, A., Curti, B., and Vanoni, M.A. (1999). Identifying and quantitating FAD and FMN in simple and in iron-sulfur-containing flavoproteins. *Methods in Molecular Biology (Clifton, N.J.)* 131, 9–23.

[30] Harrison, S.T.L. (2011). Cell Disruption. In Comprehensive Biotechnology, Second Edition, *(Elsevier Inc.)*, pp. 619–640.

[31] Peternel, Š. (2013). Bacterial cell disruption: A crucial step in protein production. *New Biotechnology* 30, 250–254.

[32] Bornhorst, J.A., and Falke, J.J. (2000). Purification of proteins using polyhistidine affinity tags. *Methods in Enzymology* 326, 245–254.

[33] Hausinger, R.P., Honek, J.F., and Walsh, C. (1986). [33] Separation of Flavins and Flavin Analogs by High-Performance Liquid Chromatography. *Methods in Enzymology* 122, 199–209.

[34] Blake, R., O'Brien, T.A., Gennis, R.B., and Hager, L.P. (1982). Role of the divalent metal cation in the pyruvate oxidase reaction. *Journal of Biological Chemistry* 257, 9605–9611.

[35] Yeh, J.I., Du, S., Tortajada, A., Paulo, J., and Zhang, S. (2005). Peptergents: Peptide detergents that improve stability and functionality of a membrane protein, glycerol-3-phosphate dehydrogenase. *Biochemistry* 44, 16912–16919.

[36] Krungkrai, J., Cerami, A., and Henderson, G.B. (1991). Purification and Characterization of Dihydroorotate Dehydrogenase from the Rodent Malaria Parasite *Plasmodium berghei*. *Biochemistry* 30, 1934–1939.

[37] Knecht, W., Henseling, J., and Löffler, M. (2000). Kinetics of inhibition of human and rat dihydroorotate dehydrogenase by atovaquone, lawsone derivatives, brequinar sodium and polyporic acid. *Chemico-Biological Interactions 124*, 61–76.

[38] Zameitat, E., Freymark, G., Dietz, C.D., Löffler, M., and Bölker, M. (2007). Functional expression of human dihydroorotate dehydrogenase (DHODH) in *pyr4* mutants of *Ustilago maydis* allows target validation of DHODH inhibitors in vivo. *Applied and Environmental Microbiology* 73, 3371–3379.

[39] Sen, R., and Dasgupta, D. (2003). Simple Fluorescence Assays Probing Conformational Changes of *Escherichia coli* RNA Polymerase during Transcription Initiation. *Methods in Enzymology* 370, 598–605.

[40] Changeux, J.P. (2012). Allostery and the Monod-Wyman-Changeux Model After 50 Years. *Annual Review of Biophysics* 41, 103–133.

[41] Zhang, X., Bayles, K.W., and Luca, S. (2017). *Staphylococcus aureus* CidC Is a Pyruvate:Menaquinone Oxidoreductase. *Biochemistry* 56, 4819–4829.

[42] Sena, F.V., Batista, A.P., Catarino, T., Brito, J.A., Archer, M., Viertler, M., Madl, T., Cabrita, E.J., and Pereira, M.M. (2015). Type-II NADH: Quinone oxidoreductase from *Staphylococcus aureus* has two distinct binding sites and is rate limited by quinone reduction. *Molecular Microbiology* 98, 272–288.

[43] Monk, I.R., and Foster, T.J. (2012). Genetic manipulation of *Staphylococci*-breaking through the barrier. *Frontiers in Cellular and Infection Microbiology* 2, 49.

[44] Monk, I.R., Shah, I.M., Xu, M., Tan, M.W., and Foster, T.J. (2012). Transforming the untransformable: Application of direct transformation to manipulate genetically *Staphylococcus aureus* and *Staphylococcus epidermidis*. *MBio 3*.

[45] Kato, F., and Sugai, M. (2011). A simple method of markerless gene deletion in *Staphylococcus aureus. Journal of Microbiological Methods* 87, 76–81.

[46] Arnaud, M., *Chastanet*, A., and Débarbouillé, M. (2004). New vector for efficient allelic replacement in naturally nontransformable, low-GC-content, gram-positive bacteria. *Applied and Environmental Microbiology* 70, 6887–6891.

[47] Prax, M., Lee, C.Y., and Bertram, R. (2013). An update on the molecular genetics toolbox for *staphylococci*. *Microbiology (United Kingdom)* 159, 421–435.

[48] Augustin, J., and Götz, F. (1990). Transformation of *Staphylococcus epidermidis* and other staphylococcal species with plasmid DNA by electroporation. *FEMS Microbiology Letters* 66, 203–207.

[49] Bae, T., and Schneewind, O. (2006). Allelic replacement in *Staphylococcus aureus* with inducible counter-selection. *Plasmid* 55, 58–63.

7. Supplementary materials

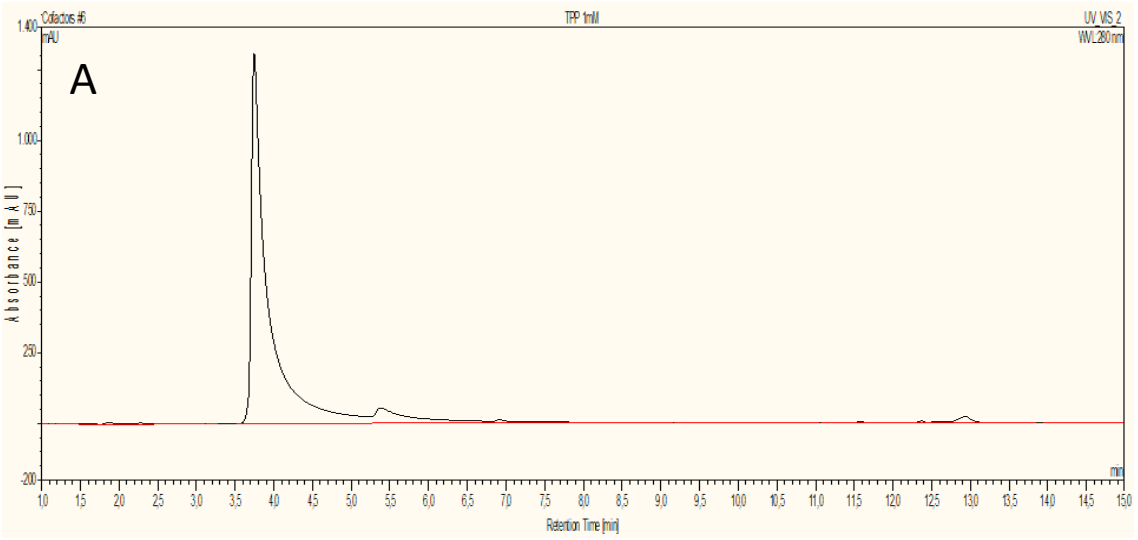

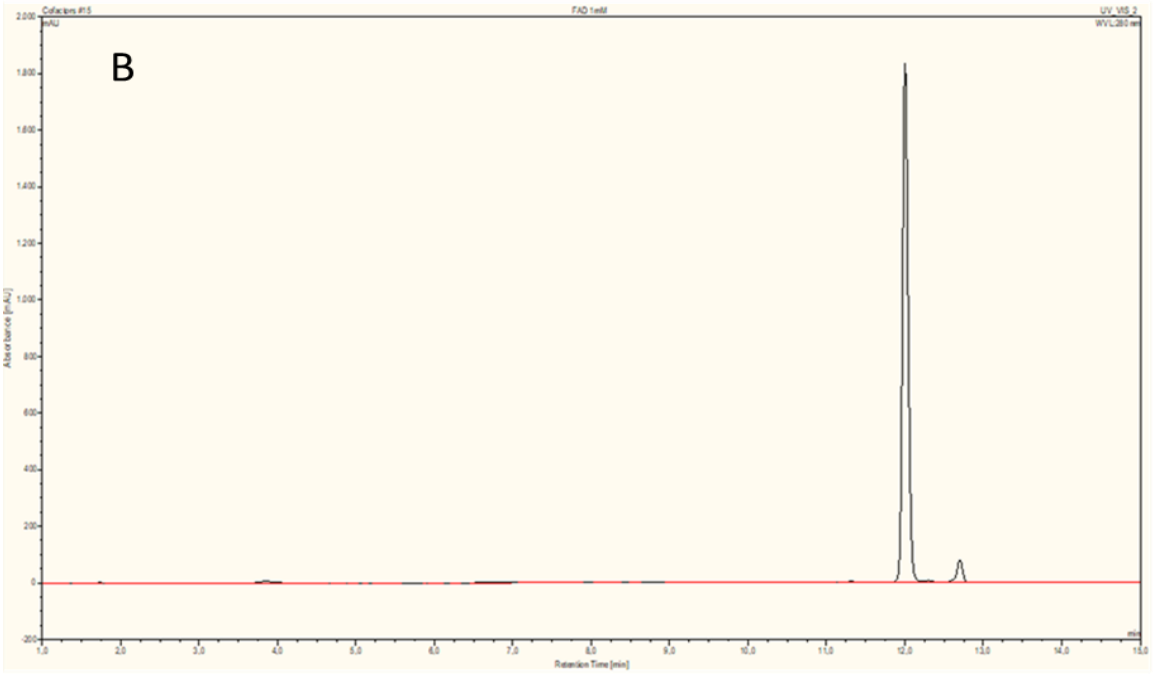

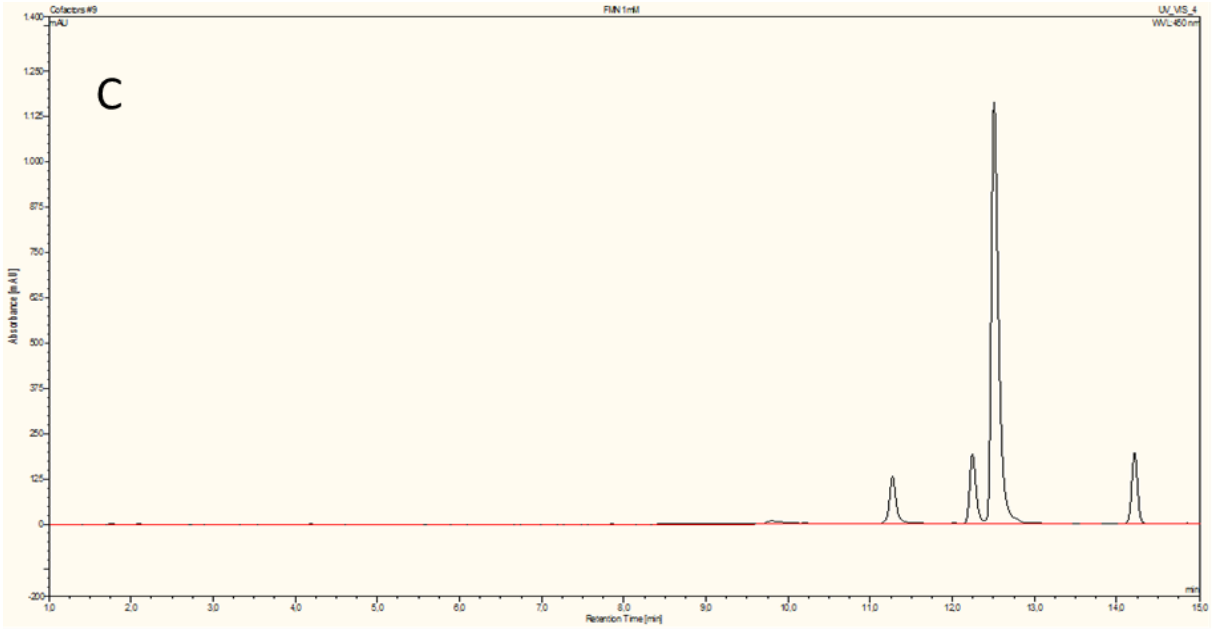
C
Cofactors #9
FUN 1ml
UV_VIS_4
mAU
WVL:450 nm
Absorbance [mAU]
Retention Time [min]
min

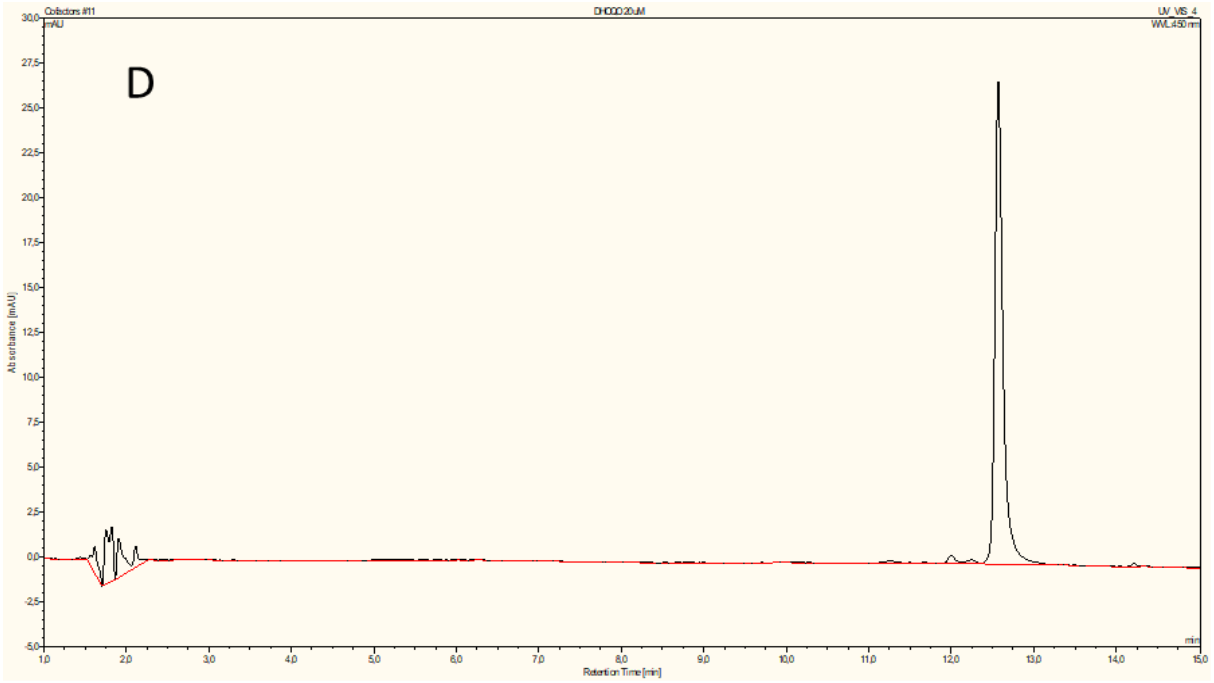
D
Cofactors #11
DHODD 20uM
UV_VIS_4
mAU
WVL:450 nm
Absorbance [mAU]
Retention Time [min]
min

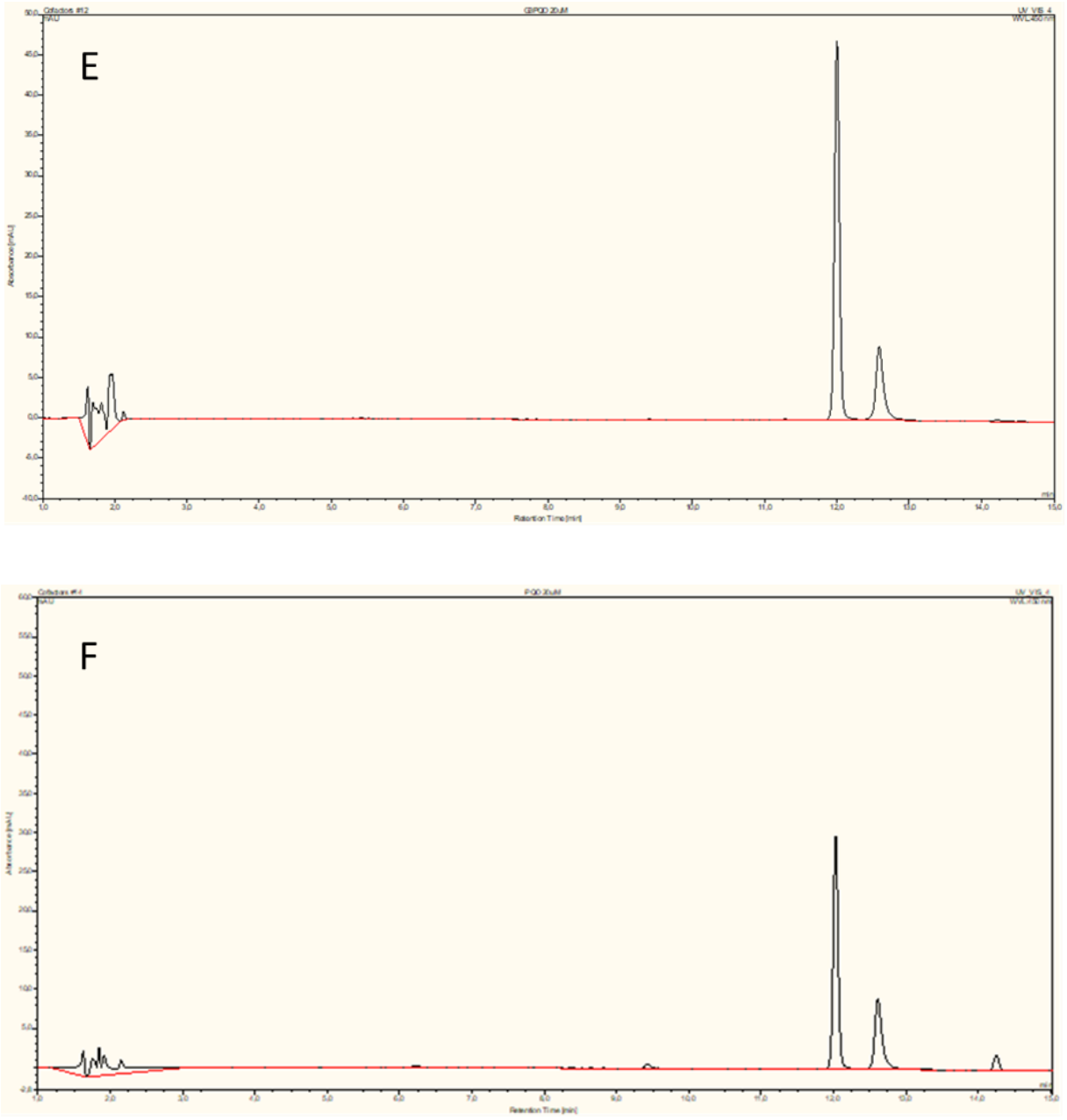

Figure 7.1- Chromatograms of the cofactor identification. FAD, FMN and TPP were injected in a Luna C18 column 3 µm (150 × 4.60 mm) operated in a HPLC system. The column was equilibrated with buffer A, 5 mM ammonium sulfate. The elution was performed using the buffer B, 5 % methanol. The sample was eluted in the same buffer with an isocratic gradient from 10 to 80 % of methanol at 1 mL $^{-1}$ min $^{-1}$. Solutions of 100 µM of FAD, FMN and TPP were used as standards. A- chromatogram of TPP injection; B- chromatogram of FAD injection; C-chromatogram of FMN injection; D- supernatant of DHOQO injection; E- supernatant of G3PQO injection; F- supernatant of PQO injection

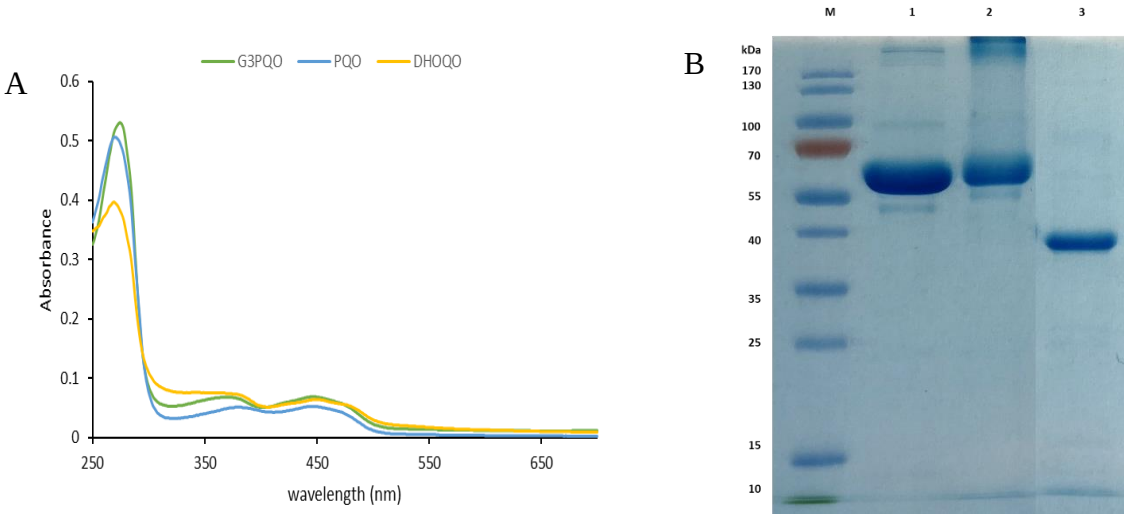

Figure 7.2- A- UV-Visible spectras of 6 µM of DHOQO, G3PQO and PQO in 50 mM K_2HPO_4/KH_2PO_4 pH 7.0, 250 mM NaCl buffer. B- The SDS-PAGE gel of the DHOQO, G3PQO and PQO from *Staphylococcus aureus* . Lane 1- G3PQO, Lane 2- PQO and Lane 3- DHOQO. PeqGOLD protein-Marker iv was used as protein mass marker ranging from 10 to 170 kDa.

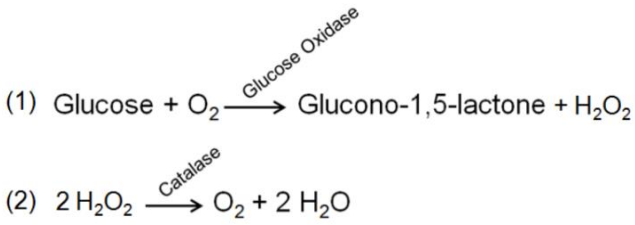

Figure 7.3-Schematic representation of mechanism of action of Scavenging system. Representation of the reaction performed by Glucose oxidase and Catalase that allow the O_2 free conditions in the performed assays. 1- Glucose oxidase consumes glucose and oxygen to form oxygen peroxide. 2- Catalase consumes the formed oxygen peroxide to form water.

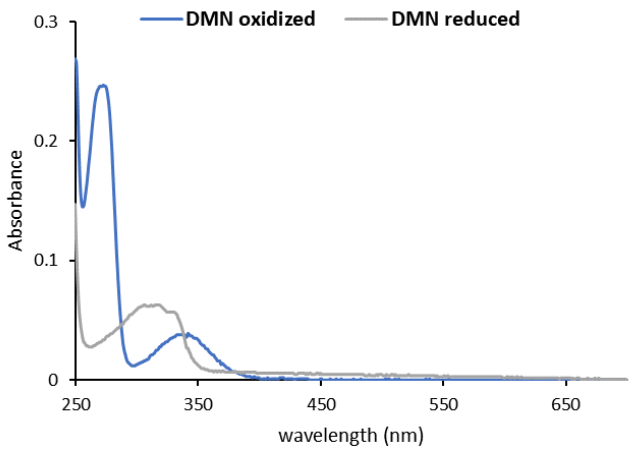

Figure 7.4 - Oxidized and reduced DMN spectras. The reduction of the quinone was achieved by the addition of sodium dithionite in 100 mM K_2HPO_4/KH_2PO_4 pH 7.0, 250 mM NaCl buffer.

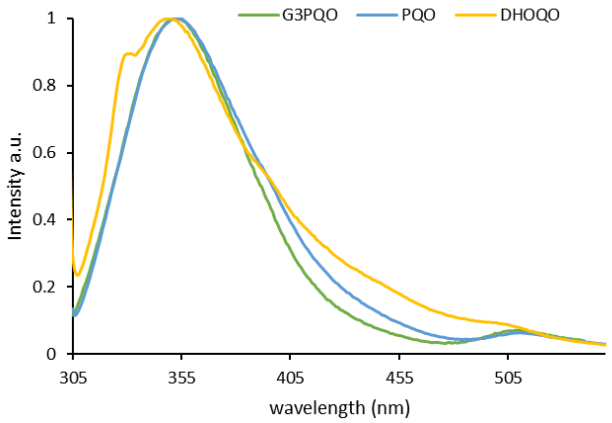

Figure 7.5- Emission spectras of the 2 µM of DHOQO, G3PQO and PQO with excitation wavelength at 295 nm in 50 mM K_2HPO_4/KH_2PO_4 pH 7.0, 250 mM NaCl buffer.

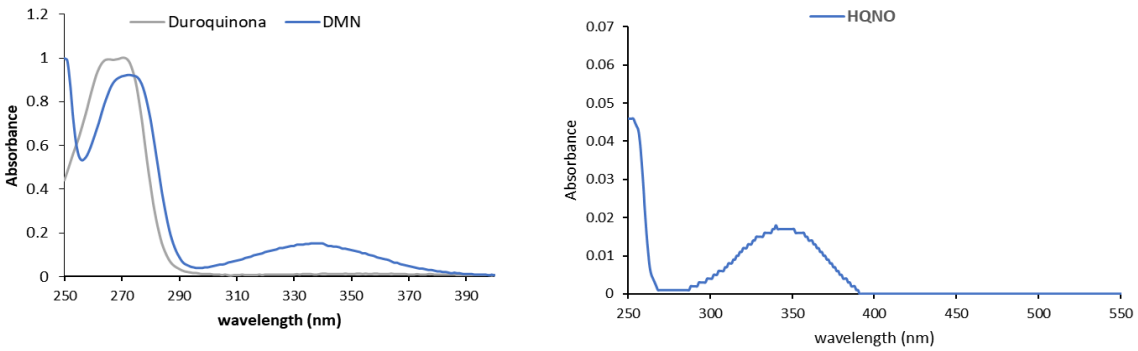

Figure 7.6 -UV- Visible spectras of 20 µM of DMN, duroquinone and HQNO in 50 mM K_2HPO_4/KH_2PO_4 pH 7.0, 250 mM NaCl buffer.

Table 7.1-Primer name, sequence, restriction enzyme, melting temperature, length of the up, down and overlap fragments and overlapping temperature of annealing of each pair of primers used in the construction of the knockout mutants. The highlighted region are the restriction sites.

Primer name	Sequence 5´-3´	Enzyme	Tm (°C)	Ta (°C)	bp	Overlap PCR (°C)	Overlap PCR (bp)
P1-DHOQO-KO	CG**CCCGGG**TCACTTTTATTGTAACTCAACCTT	XmaI	56	56.4	1274	70.1	2555
P2-DHOQO-KO	ACTATGTTGGAGAGTATGCTCCTATTTCATTATA		52.4				
P3-DHOQO-KO	TACTCTCCAACATAGTCAAATAATACTTTAA	MluI	54.2	58.1	1292		
P4-DHOQO-KO	CC**ACGCGT**ATGACAAGGTGTTGAAGAAATTAAT		57				
P1-G3PQO-KO	CG**CCCGGG**TTAGAGATAAGACAGGATTACTT	XmaI	53.3	57.3	1311	68.9	2599
P2-G3PQO-KO	TATGATTGTACAAATTAATCCAAAACGCCTCCTAAA		55.6				
P3-G3PQO-KO	TTAATTTGTACAATCATAAACTGGTG	SalI	55.8	59.1	1305		
P4-G3PQO-KO	CG**GTCGAC**TCATCAGGATTCAAGATATCAATT		55.3				
P1-PQO-KO	GC**CCCGGG**AAGCACTCATTATTTAAGGC	XmaI	52.9	57	1326	68	2659
P2-PQO-KO	TATTACTAATAGCCTCCCTTTCTG		56.6				
P3-PQO-KO	GAGGCTATTAGTAATATTTAGATCAAATTCCACC	BamHI	48.2	52.5	1343		
P4-PQO-KO	CC**GGATCC**TCCTGCTGATAACATTAAAC		52.3				

Table 7.2 - DNA concentration and ratios A260/A280 and A260/A230 of the extracted plasmid (pMAD+ insert) from the positive colonies of *E. coli* DC10B to the presence of the construct of interest for DHOQO and G3PQO

	DHOQO KO			**G3PQO KO**		
Colony	**[DNA] ng/µL**	**A260/A280**	**A260/A230**	**[DNA] ng/µL**	**A260/A280**	**A260/A230**
a	167.8	1.86	2.01	232.9	1.84	2.09
b	131.8	1.77	1.59	260.3	1.87	2.18
c	128.8	1.83	1.72	239.4	1.87	2.29